

การพัฒนาอะลูมินาเซรามิกโปร่งใสที่มีผลึกระดับนาโน : ผลของการขึ้นรูปและภาวะการเผาผลึก



นายสุนทร แทนสูงเนิน

สถาบันวิทยบริการ

จุฬาลงกรณ์มหาวิทยาลัย

วิทยานิพนธ์นี้เป็นส่วนหนึ่งของการศึกษาตามหลักสูตรปริญญาวิทยาศาสตรมหาบัณฑิต

สาขาวิชาเทคโนโลยีเซรามิก ภาควิชาวัสดุศาสตร์


คณะวิทยาศาสตร์ จุฬาลงกรณ์มหาวิทยาลัย

ปีการศึกษา 2548

ISBN 974-17-4766-7

ลิขสิทธิ์ของจุฬาลงกรณ์มหาวิทยาลัย

DEVELOPMENT OF TRANSPARENT NANO-CRYSTALLINE ALUMINA CERAMIC: EFFECTS OF  
FORMING AND SINTERING CONDITIONS



Mr.Soontorn Tansungnoen

สถาบันวิทยบริการ  
จุฬาลงกรณ์มหาวิทยาลัย

A Thesis Submitted in Partial Fulfillment of the Requirements  
for the Degree of Master of Science Program in Ceramic Technology

Department of Materials Science

Faculty of Science

Chulalongkorn University

Academic Year 2005

ISBN 974-17-4766-7



สุนทร แทนสูงเนิน : การพัฒนาอะลูมินาเซรามิกโปร่งใสที่มีผลึกระดับนาโน : ผลของการขึ้นรูปและภาวะการเผาผนึก. (DEVELOPMENT OF TRANSPARENT NANO-CRYSTALLINE ALUMINA CERAMIC: EFFECTS OF FORMING AND SINTERING CONDITIONS)

อ. ที่ปรึกษา : ศาสตราจารย์ ดร. ชิกทากะ วาคะ, อ.ที่ปรึกษาร่วม : ดร. ภาวดี อังค์วัฒน์,  
88 หน้า. ISBN 974-174-766-7.

งานวิจัยนี้มุ่งเน้นในการพัฒนาเทคโนโลยีในการสังเคราะห์อะลูมินาเซรามิกโปร่งใสโดยการควบคุมขนาดเกรนของอะลูมินาเซรามิกให้อยู่ในระดับนาโน ในการทดลองได้ศึกษาผลของการขึ้นรูปและภาวะการเผาผนึกต่อความโปร่งใสและขนาดเกรนของอะลูมินาเซรามิก ในงานวิจัยได้ใช้ผงอะลูมินาเกรด TMDA ซึ่งมีขนาดอนุภาคเล็กในระดับนาโน โดยการผสมผงอะลูมินากับแมกนีเซียมออกไซด์ 0-0.1 เปอร์เซ็นต์โดยน้ำหนัก แล้วขึ้นรูปโดยการให้ความดันทุกทิศทางแบบเย็นและการหล่อแบบเจล แล้วเผาผนึกในบรรยากาศปกติและสุญญากาศที่อุณหภูมิ 1250-1550 องศาเซลเซียส เป็นเวลา 2 ชั่วโมง หลังจากนั้นทำการเผาผนึกโดยการให้ความดันทุกทิศทางแบบร้อนที่อุณหภูมิ 1250-1300 องศาเซลเซียส เป็นเวลา 2 ชั่วโมง ภายใต้ความดันก๊าซอาร์กอน 150 เมกะพาสคัล

ผงอะลูมินาที่ผสมกับแมกนีเซียมออกไซด์ แล้วถูกนำมาขึ้นรูปโดยการให้ความดันทุกทิศทางแบบเย็นและเผาผนึกในสุญญากาศที่อุณหภูมิ 1450 ถึง 1550 องศาเซลเซียสจะโปร่งแสง ในกรณีที่ไม่เติมแมกนีเซียมออกไซด์จะทึบแสง และถ้าเผาผนึกในบรรยากาศปกติทั้งที่เดิมและไม่เติมแมกนีเซียมออกไซด์จะทึบแสง การเผาผนึกที่อุณหภูมิต่ำกว่า 1350 องศาเซลเซียสในทั้งสองบรรยากาศจะได้อะลูมินาเซรามิกที่มีเกรนอยู่ในระดับนาโน อะลูมินาเซรามิกที่เผาผนึกในบรรยากาศปกติที่อุณหภูมิ 1300 องศาเซลเซียส และนำไปเผาผนึกอีกครั้งโดยการให้ความดันทุกทิศทางแบบร้อนจะโปร่งใส ในขณะที่การเผาผนึกในสุญญากาศจะโปร่งแสง การขึ้นรูปโดยการหล่อแบบเจลสามารถเตรียมชิ้นงานที่มีลักษณะโปร่งใสได้เช่นกัน แต่ความโปร่งใสยังน้อยกว่าการขึ้นรูปแบบการให้ความดันทุกทิศทางแบบเย็น

ภาควิชาวัสดุศาสตร์  
สาขาวิชา เทคโนโลยีเซรามิก  
ปีการศึกษา 2548

ลายมือชื่อนิสิต..... *Somborn T.*  
ลายมือชื่ออาจารย์ที่ปรึกษา..... *S. Wada*  
ลายมือชื่ออาจารย์ที่ปรึกษาร่วม..... *[Signature]*

# # 4672452523 : MAJOR CERAMIC TECHNOLOGY

KEY WORD: TRANSPARENT ALUMINA / FORMING / SINTERING

SOONTORN TANSUNGNOEN : DEVELOPMENT OF TRANSPARENT NANO-CRYSTALLINE ALUMINA CERAMIC: EFFECTS OF FORMING AND SINTERING CONDITIONS. THESIS ADVISOR : PROF.SHIGETAKA WADA, Ph.D., THESIS COADVISOR : PAVADEE AUNGKAVATTANA, Ph.D., 88 pp. ISBN 974-17-4766-7.

The objective of this study was to develop a technology for synthesizing transparent polycrystalline alumina ceramic by controlling the grain size in the range of nanometer level. The experiment concentrated on the effects of forming and sintering conditions on the transparency and grain size. Alumina powder (TMDA) of nanometer size was used as starting material. The alumina powder was mixed with MgO ranging from 0-0.1 wt%. Alumina bodies were formed by both cold isostatic press (CIP) and gel casting using agar as the gelling additive. The green bodies were sintered at 1250 to 1550°C for 2 h both in air and under vacuum followed by hot isostatic pressing (HIP) at 1250 and 1300°C for 2 h under Ar pressure of 150 MPa.

Alumina ceramic doped with MgO formed by CIP method and sintered under vacuum at 1450 to 1550°C was translucent, while MgO-free alumina ceramic was opaque. On the other hand, both MgO-free and MgO doped alumina ceramic sintered in air were opaque. Nanometer size grain was achieved at the sintering temperature lower than 1350°C. Specimen pre-sintered in air atmosphere followed by hot isostatic pressing became transparent. On the other hand, specimen pre-sintered under vacuum was translucent and still showed gray color. Alumina ceramics formed by gel casting showed transparency. However, alumina ceramics formed by CIP method showed transparency better than that formed by gel casting method.

Department Materials Science  
Field of study Ceramic Technology  
Academic year 2005

Student's signature.....*Somborn T.*  
Advisor's signature.....*S. Wada*  
Co-advisor's signature.....*PAVADEE AUNGKAVATTANA*

## ACKNOWLEDGEMENTS

I would like to express my deep gratitude to my advisor, Professor Dr. Shigetaka Wada, for his encouragement, consistent guidance and for all that I have learnt from him throughout this research and any thing. His advises never failed to inspire the good idea and my motivation. I would like to extend my gratitude to my thesis co-advisor, Dr.Pavadee Aungkavattana, who gave me good advices and encouragement.

I would like to acknowledge Associate Professor Dr. Supatra Jinawath, Associate Professor Dr. Tawatchai Charinpanitkul and Mr. Nirut Wangmuklang for them helpful suggestions.

I would like to thank the Thailand Graduate Institute Science and Technology (TGIST), National Nanotechnology Center (NANOTEC), National Science and Technology Development Agency (NSTDA) and Research Unit of Advance Ceramic (RU of Advance ceramic) Chulalongkorn University for financial support.

I would like to thank Thailand Institute of Science and Technology Research (TISTR), and Scientific and Technological of Research Equipment Center (STREC) for equipment support.

Thanks to all my friends at the Department of Materials Science for their friendship and supports.

Finally, I would like to express my gratitude to my family especially my father, mother and my wife for their loves, understanding and encouragement.

จุฬาลงกรณ์มหาวิทยาลัย

## CONTENTS

	Page
Abstract (Thai).....	iv
Abstract (English).....	v
Acknowledgements.....	vi
Contents.....	vii
Lists of Tables.....	x
Lists of Figures.....	xi
Chapter I Introduction.....	1
Chapter II Literature Reviews.....	3
2.1 Transparency, translucency and opaque.....	3
2.2 Transparent alumina.....	4
2.2.1 Sources of light scattering.....	4
2.2.2 Grain-boundary reflection.....	5
2.2.3 Grain boundary refraction.....	6
2.2.4 Effect of grain size on transmittance.....	6
2.3 Transparent alumina ceramic fabrication route.....	7
2.3.1 Forming technology.....	8
2.3.2 Sintering technology.....	9
2.4 Literature surveys of transparent polycrystalline alumina.....	10
Chapter III Experimental procedures.....	14
3.1 Raw materials and characterization.....	14
3.1.1 Starting raw materials.....	14
3.1.2 Raw material characterization.....	15
3.1.2.1 Particle size distribution .....	15
3.1.2.2 Microstructure observation by SEM.....	15
3.1.2.3 Specific Surface Area.....	15
3.1.2.4 Thermal behavior of $Mg(NO_3)_2 \cdot 6H_2O_{(s)}$ and agar...15	
3.2 Composition and Preparation of alumina green body.....	16
3.2.1 Preparation of green body by cold isostatic press method.....	16

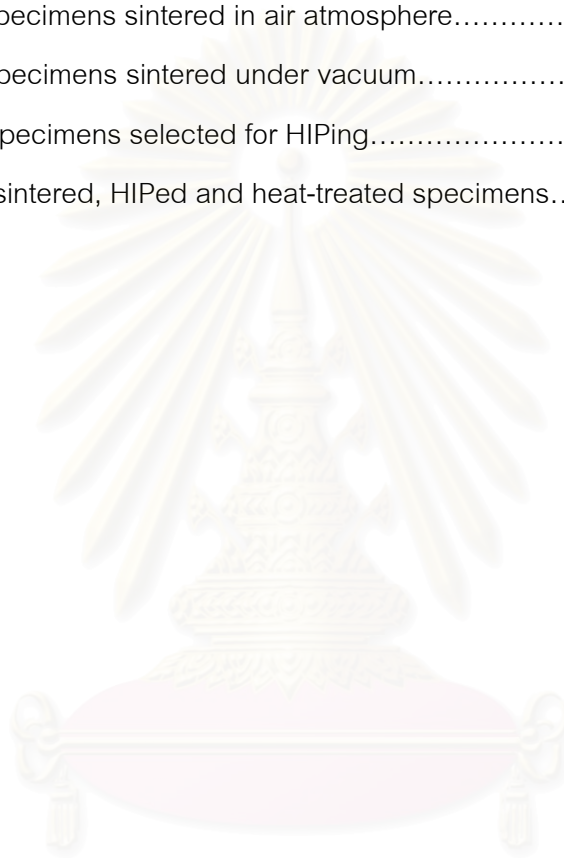
	Page
3.2.2 Preparation of green body by gel casting method.....	17
3.3 Viscosity of slurry.....	22
3.4 Characterization of green body.....	22
3.4.1 Drying shrinkage.....	22
3.4.2 Bulk density.....	22
3.5 Characterization of sintered specimen.....	22
3.5.1 Bulk density.....	22
3.5.2 Microstructure.....	23
3.5.3 Transmittance.....	23
<b>Chapter IV Results and discussions.....</b>	<b>25</b>
4.1 Raw materials characterization.....	25
4.1.1 Particle size distribution.....	25
4.1.2 Shape of alumina powder.....	26
4.1.3 Thermal behavior of $Mg(NO_3)_2 \cdot 6H_2O_{(s)}$ and agar.....	27
4.2 Cold press followed by CIP method.....	28
4.2.1 Characterization of green body.....	28
4.2.2 Characterization of sintered specimens.....	30
4.2.2.1 Density.....	30
4.2.2.2 Colors.....	31
4.2.2.3 Microstructure of sintered specimens.....	35
4.2.2.4 Transparency.....	39
4.2.3 Sinter-HIP.....	42
4.2.3.1 Density.....	43
4.2.3.2 Colors.....	45
4.2.3.3 Microstructure.....	46
4.2.3.4 Transparency.....	47
4.3 Gel-casting method.....	48
4.3.1 Characterization of slurry.....	48



	Page
4.3.2 Characterization of green bodies.....	51
4.3.3 Characterization of sintered specimens.....	57
4.3.4 Sinter-HIP.....	58
Chapter V Conclusions.....	61
Chapter VI Future works.....	63
References.....	64
Appendices.....	68
Appendix A Density of green bodies form by biaxial press method....	69
Appendix B Density of green bodies formed by CIP method.....	70
Appendix C Bulk density, relative density, apparent porosity and water absorption of CIP specimens sintered under vacuum atmosphere.....	72
Appendix D Bulk density, relative density, apparent porosity and water absorption of CIP specimens sintered in air atmosphere.....	77
Appendix E Average grain size of sintered specimens.....	82
Appendix F Density of green bodies form by gel casting using agar as gelling additive.....	83
Appendix G Density of sintered specimens formed by gel-casting method.....	86
Appendix H. Surface roughness of specimens polished by a Japanese company.....	87
Biography.....	88

## LIST OF TABLES

	Page
Table 3.1 Raw materials used in this experiment.....	14
Table 3.2 Compositions of alumina powder with MgO.....	16
Table 3.3 Contents of agar and solid loading Al <sub>2</sub> O <sub>3</sub> in the slurries.....	19
Table 4.1 Color of specimens sintered in air atmosphere.....	33
Table 4.2 Color of specimens sintered under vacuum.....	34
Table 4.3 Sintered specimens selected for HIPing.....	41
Table 4.4 Colors of sintered, HIPed and heat-treated specimens.....	44



สถาบันวิทยบริการ  
จุฬาลงกรณ์มหาวิทยาลัย

## LIST OF FIGURES

	Page
Fig. 2.1 Various interactions between radiation and solid.....	4
Fig. 2.2 Illustration of the most important light-scattering mechanisms in polycrystalline alumina.....	5
Fig. 2.3 The real in-line transmittance (RIT) of alumina ceramic measured at wavelength 645 nm as a function of the mean grain size.....	7
Fig. 2.4 History of the progress of technology to produce transparent polycrystalline alumina from 1960s to 2000s.....	13
Fig. 3.1 Flow chart of green body preparation by cold isostatic pressing process.....	20
Fig. 3.3 Flow chart of green body preparation by gel casting process.....	21
Fig. 4.1 Particle size distribution of TMDA alumina powder.....	25
Fig. 4.2 SEM micrograph of TMDA powder.....	26
Fig. 4.3 Thermal behavior of (a) $Mg(NO_3)_2 \cdot 6H_2O$ and (b) agar powder analyzed by TGA/DTA technique.....	28
Fig. 4.4 Densities of green bodies formed by cold press and cold isostatic press methods.....	29
Fig. 4.5 SEM micrograph of fractured surface of green body (TR3) formed by cold isostatic press method.....	30
Fig. 4.6 Relationship between relative density and sintering temperature of alumina compacts formed by CIP and sintered (a) under vacuum and (b) in air atmosphere.....	31
Fig.4.7 Relationship between average grains size of alumina versus sintering temperature both in air atmosphere and under vacuum.....	35
Fig.4.8 SEM micrographs of specimens sintered at (a) 1350 and (b) 1550°C for 2 h under vacuum.....	36
Fig. 4.9 SEM micrographs of specimens sintered at 1350°C for 2 h (a) in air and (b) under vacuum.....	37

Fig. 4.10 Transparency of TR3 sintered at 1550°C for 2 h (a) in air atmosphere and (b) under vacuum. Both specimens are 1 mm thick and polished on both side.....	39
Fig. 4.11 Transparency and microstructure of (a) TR1 and (b) TR3 sintered at 1550°C for 2 h under vacuum.....	40
Fig. 4.12 Relative densities of specimens before and after HIPing at condition A, (1250°C,2h).....	42
Fig. 4.13 Relative densities of specimens before and after HIPing at condition B (1300°C, 2 h).....	43
Fig. 4.14 SEM micrograph of TR3 (a) pre-sintered in air and (b) under vacuum followed by HIPing at 1300°C for 2 h under Ar pressure of 150 MPa.....	45
Fig. 4.15 Optical micrographs of specimens (a) pre-sintered in air and (b) under vacuum followed by HIPing at condition B (1300°C, 2 h). All specimens were ground to 1 mm thick and polished on both side.....	46
Fig.4.16 Relationship between wavelength and transmittance (%T) of HIPed specimens, the specimens prepared by pre-sintered at 1300°C for 2 h both in (A) air and (V) vacuum atmosphere followed by HIPing at 1300°C for 2 h under Ar pressure of 150 MPa.....	47
Fig. 4.17 Relationship between viscosity and amount of dispersant (Aron, A6114) of alumina slurries.....	48
Fig. 4.18 Change of pH and viscosity for 70 wt% alumina slurry without and with $Mg(NO_3)_2 \cdot 6H_2O$ .....	49
Fig. 4.19 Evolution of viscosity on cooling of 2 wt% agar solution.....	50
Fig. 4.20 Viscosity of alumina slurries as the function of total amount of agar, 0.1, 0.2 and 0.3 wt% based on dry solid, 100s <sup>-1</sup> and 45°C.....	51
Fig. 4.21 Pictures of green bodies formed by gel casting method.....	52
Fig. 4.22 Shrinkage of gel-cast bodies after drying at 105°C.....	53

	Page
Fig. 4.23 Density of gel-cast green bodies of composition G2-G9 dried in route1 and 2.....	54
Fig. 4.24 Pictures of gel-cast bodies were dried in route 1 and 2.....	55
Fig. 4.25 SEM micrographs of fractured surface of green body formed by gel-casting method.....	56
Fig. 4.26 Densities of sintered specimens formed by gel-casting method.....	57
Fig. 4.27 SEM micrograph of G7 pre-sintered at 1300°C for 2 h in air atmosphere followed by HIPing at condition B. (1300°C for 2 h).....	58
Fig.4.28 Optical micrographs and microstructure of HIPed specimens formed by gel casting and CIP methods. (the thickness were 0.8 mm.) The distance between disc and printed paper was 1 cm.....	59
Fig.4.29 Relationship between wavelength and transmittance (%T) of HIPed specimens formed by both gel-casting and CIP methods.....	60

## CHAPTER I

### INTRODUCTION

Alumina ( $\text{Al}_2\text{O}_3$ ) ceramics have been widely used as an integrated circuit (IC) substrate, the insulator for spark plug, a media ball, crucibles, and the envelope of high pressure sodium lamp, due to its high electrical resistance, good thermal conductivity, high melting point, excellent chemical resistance, high hardness and high mechanical strength [1-4].

Alumina ceramics are usually poly-crystalline and not transparent. Transparent alumina ceramic can be synthesized either in single crystal (SCA) or polycrystalline forms (PCA)[5]. SCA (single crystal alumina) is used as highly transparent material for many industrial and military applications, such as optical windows for laser, armor part, IR-dome for infrared missile guidance system and jewelry. PCA (polycrystalline alumina) has been available for optical application since early 1962 when Coble[6] invented translucent alumina, which was composed of micrometer-sized grains and not transparent, but translucent. Recently, it has been reported that transparent alumina with nano-meter sized grain can be made [7-11].

$\text{Al}_2\text{O}_3$  has no color when it is chemically pure. However, the color changes to pink or red when small amount of Cr-ion is added and blue when Fe-ion is contaminated. If beautiful colors could be added to PCA, it would become a kind of jewelry. The advantage of such invented ceramic is that its size and shape can be formed artificially. If we could develop technology for doping color into such transparent ceramic, we would be able to produce the statue of Buddha, the statue of freedom or any other complicated figures in various colors. The development of PCA would actuate a new world of artificial precious stones, which could be differentiated from that of natural jewelry and in turn could help increase the nation's benefits. Compared to SCA, the cost to manufacture PCA is much lower, and it is easier to produce in large size and complicated shape.

From the background above mentioned, we are interested in the development of technology to synthesize a transparent polycrystalline alumina ceramic for jewelry industry.

Normally the light transmission of PCA is relatively small in contrast to SCA, which shows a complete transparency. The low light transmission of PCA is caused by scattering of light at grain boundaries and residual pores[4]. Thus, transparency of PCA can be increased by complete eliminating of the residual porosity, and reducing the grain size to submicron or nanometer level [8]. Key factors to obtain this characteristic are using high purity and fine particle size alumina powder (sub-micrometer or nanometer level) with a small amount of MgO, forming green bodies with high density and high homogeneity particle packing, and sintering in hydrogen or vacuum atmosphere followed by hot isostatic pressing (HIP). Many studies have been conducted on technologies for synthesizing transparent alumina ceramic. However, there have been very few reports of clear dependency of those conditions on the product characteristic.

In this research, we aimed to concentrate on the increasing transmittance of alumina ceramic by reducing alumina grain to nanometer level. Forming and sintering conditions were studied intending to attain nanometer size grain.

**The objectives of this research are as follows:**

1. To develop a technology for synthesizing transparent polycrystalline alumina ceramic.
2. To investigate the relationship between forming and sintering conditions on the grain size of alumina.
3. To investigate the relationship between the alumina grain size and transmittance.

## CHAPTER II LITERATURE REVIEWS

### 2.1 Transparency, translucency and opaque

When beam of light or electromagnetic (EM) radiation impinges on the solid (Fig. 2.1.), several things happen. Some of light radiation may be transmitted through the medium, some will be absorbed, and some will be reflected at the interface between the two media. The intensities  $I_0$  of the incident beam to the surface of the solid medium must equal to the sum of the intensity of the transmitted, absorbed, and reflected beams, denoted as  $I_T$ ,  $I_R$ , and  $I_A$ , respectively,

$$I_0 = I_T + I_R + I_A \dots\dots\dots(2.1)$$

An alternate form of Equation 2.1 is

$$1 = T + R + A \dots\dots\dots(2.2)$$

where  $T$ ,  $R$  and  $A$  represent the transmissivity ( $I_T/I_0$ ), reflectivity ( $I_R/I_0$ ) and absorptivity ( $I_A/I_0$ ), respectively, or the fractions of incident light that are transmitted, absorbed, and reflected by a material; their sum must equal unity, since all the incident light is either transmitted, absorbed, or reflected.

Materials that are capable of transmitting light with relatively little absorption and reflection are **transparent**, one can see through them. **Translucent** materials are those that light is transmitted diffusely through the interior; that is, light is scattered within the interior to the degree that objects are not clearly distinguishable when viewed through a specimen of the material. Materials that are impervious to the transmission of visible light are termed **opaque**.



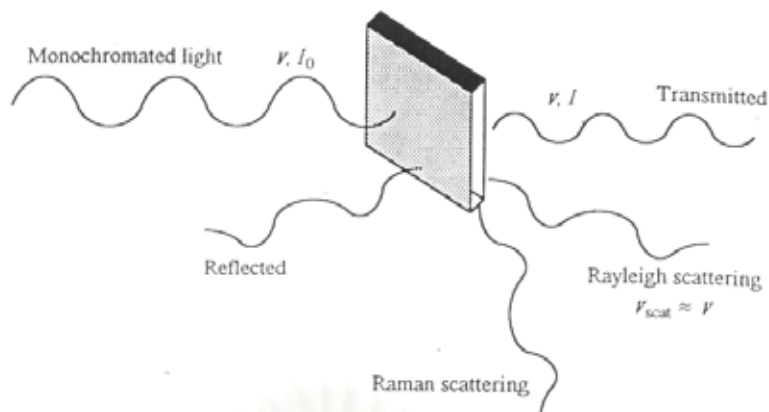


Fig. 2.1 Various interactions between radiation and solid[12].

## 2.2 Transparent alumina

There are many possible factors affecting the transparency of PCA and can be found in the literatures[13,14]. In these papers, sources of light scattering such as grain boundary reflection, refraction in  $\text{Al}_2\text{O}_3$  grain and effect of grain size on transparency are to be described.

### 2.2.1 Sources of light scattering [8]

The most important origins of light scattering in high-purity PCA are rough surfaces, pores, and grain boundaries. The light scattering mechanism is schematically illustrated in Fig.2.2. Light scattering at the surfaces of the second phases (inclusions) can be neglected in high-purity PCA. Even for MgO-doped PCA, it has no significant effect of MgO on the optical properties of PCA up to MgO content of 300 wt-ppm was reported. Absorption of light by high-purity PCA is generally low when it is sintered to full density, and it also can be neglected. When sample surfaces are smooth, the scattering of light at the surfaces also can be neglected, only the specular reflection at the surfaces of  $\sim 14\%$  has to be taken into account. Therefore, grain boundaries and pores remain as the most important factors for the light scattering of high-purity PCA.

The real in-line transmittance ( $RIT$ ) decreases exponentially with the sample thickness  $d$ :

$$RIT = (1 - R_s) \exp(-\gamma d) \dots\dots\dots(2.3)$$

$R_s$  describes the reflection losses at two sample surfaces ( $\sim 0.14$ ) at normal incidence.

$\gamma$  is the total scattering coefficient, which is the sum of grain-boundaries and pores.

So, the  $RIT$  is affected by material variables (via  $\gamma$  and  $R_s$ ) as well as the sample thickness.

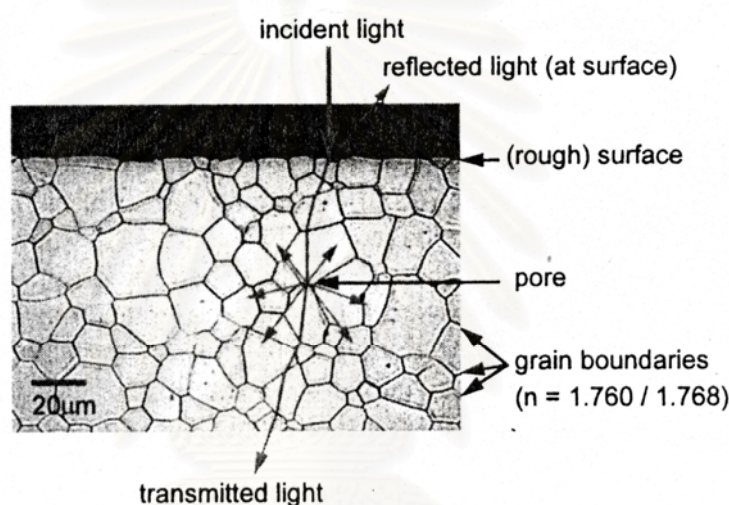


Fig. 2.2 Illustration of the most important light-scattering mechanisms in polycrystalline alumina [8].

### 2.2.2. Grain-boundary reflection

Because the crystal structure of  $\alpha\text{-Al}_2\text{O}_3$  (corundum) is hexagonal, it shows birefringence. This means that the refractive index is not the same in the crystallographic directions. For example, at wavelength of 600 nm, the refractive index of  $\text{Al}_2\text{O}_3$  is 1.768 for the ordinary ray (polarization perpendicular to the c-axis) and 1.760 for the extraordinary ray (polarization parallel to the c-axis)[15]. The refractive index different of 0.008 is virtually independent of temperature and wavelength. The birefringence leads to a discontinuity of the refractive index ( $\Delta n$ ) at the grain boundaries

if the crystallographic orientations of the neighboring grains are not the same. As in normal PCA, the grains are randomly oriented, and  $\Delta n$  at a given grain boundary should range from zero to a maximum of 0.008. Therefore, on average, the light is refracted as well as reflected at a grain boundary. However, the reflectivity of the grain boundaries is extremely low because of small  $\Delta n$ .

### 2.2.3 Grain boundary refraction

In contrast to the reflection, the refraction of light at the grain boundaries cannot be neglected in PCA. This is first shown qualitatively for large grains by simple geometrical optics. Geometrical optics can be applied when the grains are much larger than the wavelength of the light. (More exactly, the condition is  $G\Delta n > 2\pi\lambda_m$ . Here  $\lambda_m$  is the wavelength in the medium and  $G$  is the average grain size). The deviation of light beam from its original direction can be calculated using Snell's law [16].

$$n_1 \sin \theta_1 = n_2 \sin \theta_2 \dots\dots\dots(2.4)$$

where  $\theta_1$  is the angle of incidence and  $\theta_2$  the angle of the refracted ray of light. Both angles refer to the normal of the grain boundary surface. For  $\theta_1 = 45^\circ$  and  $\Delta n = 0.008$ , the deflection ( $\theta_1 - \theta_2$ ) of the light beam from its original direction is  $0.28^\circ$ . This rough calculation shows that the refraction (deflection) of light at the grain boundaries can not be neglected, especially when it is taken into account that the light beam has passed tens or hundreds of grain boundaries in a typical PCA sample, depending on grain size and sample thickness.

### 2.2.4 Effect of grain size on transmittance

Generally, when light passes through a transparent ceramic, the in-line transmittance,  $RIT$ , follows the relation in Eq. (2.3). From this equation the scattering terms depend on grain size of the specimen, wavelength, and sample thickness and it is applicable to all birefringent polycrystalline materials as long as the restrictions bound to the derivation of the Rayleigh-Gans-Debye theory.

In 2003, Apez et al.[8] early studied the effect of grain size of alumina on transmittance, *RIT* values of various samples with a thickness of 0.80 mm had been measured, using a red laser with a wavelength of 645 nm. It was found that the in-line transmittance depended on grain size and on the amount and size distribution of a few pores. The in-line transmittance rapidly increased when grain size decreased to sub-micrometer or nano-meter level as shown in Fig. 2.3.

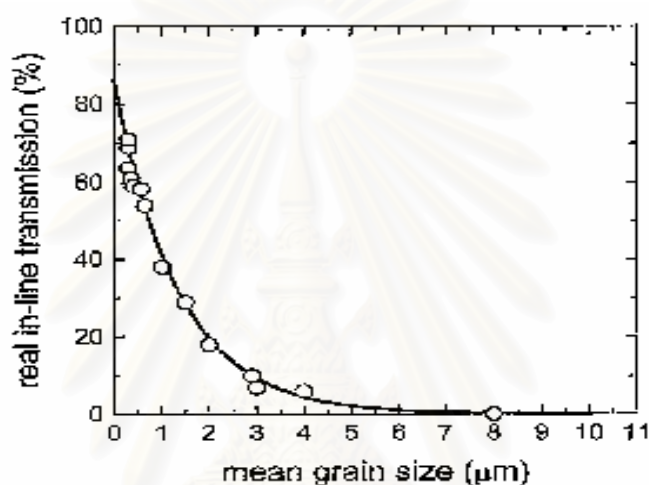


Fig. 2.3. The real in-line transmittance (RIT) of alumina ceramic measured at wavelength 645 nm as a function of the mean grain size: (O) experimental data points.

### 2.3 Transparent alumina ceramic fabrication route

Transparent polycrystalline alumina was made via powder processing using high purity and fine particle size alumina powder (sub-micrometer or nanometer level) with a small amount of MgO as grain growth inhibitor, forming green bodies with high density and high homogeneity particle packing, and sintering in hydrogen or vacuum atmosphere followed by hot isostatic pressing. In the following section, forming and sintering were examined.

### 2.3.1 Forming technology

Forming is necessary for making a powder as close together as possible in order to decrease the residual porosity by the surface tension during sintering. The choice of the forming process depends on the dimensions and shape of the part. Careful control of the density and homogeneity of green body is necessary to obtain nearly theoretical density (TD) after sintering, because large defects introduced in forming are commonly not eliminated when product is fired.

Much attention has been focused to obtain alumina ceramics with submicron microstructure in order to improve their mechanical and optical properties. For these purposes very fine and high purity powders are required. In order to sinter a submicron level grain without much grain growth by pressureless sintering, it is necessary to apply powder processing techniques like cold isostatic pressing (CIP)[10-11, 17-19], pressure filtration,[10, 11, 17] or gel-casting, [11,17] which lead to high density green bodies with good homogeneity of compaction and that allows to attain full density at low sintering temperature. In addition, the properties of a ceramic material are mainly limited by the presence of various types of defects [20]. Many of those defects arise from agglomerates present in the early stage of the processing which lead to packing inhomogeneity during forming process. Sintering tends to increase the severity of flaws present in the green body. Thus, it is very important to make a green body or pre-form with a reduced density of defects. Krell et al. [17-19] used a very fine commercial powder and obtained a sintered body with relative density of 99.2% TD. and grain size of 0.5  $\mu\text{m}$  by pressure-less sintering at various temperature depending on the type of pre-forms, i.e. pre-forms prepared by gel-casting at 1300 $^{\circ}\text{C}$ , pre-forms by pressure filtration at 1350 $^{\circ}\text{C}$ , and at 1450 $^{\circ}\text{C}$  for pre-forms by CIP. From these investigations, CIP and gel-casting were chosen for forming green body.

Cold isostatic pressing (CIP) is one of the good forming methods. It has been used in the forming of translucent alumina. It is simple and low cost operation that provides a green body of ceramic with sufficient physical strength. However, this method is not suitable to form complicated figure parts.

Gel casting (GC) is a new shaping process for advanced ceramic materials. This concept was firstly used by Golibersuch in 1962, for consolidating the slurry with metal powder by polymerization and firstly used in ceramic by Omatete in 1991 as a promising technique for complex shapes of structural ceramics [21,22]. A concentrated slurry of ceramic powder in a solution of organic monomers and dispersant is poured into a mold and then polymerized in-situ to form a green body in the shape of the mold cavity. Some organic monomers are soluble in water and become polymerized gel with increasing temperature. The particles are dispersed by electrostatic or electrosteric stabilization using a small molecular dispersant. With in-situ and permanent polymerization of monomer, the ceramic powder can retain the desired shape. Gel casting can produce near-net-shape ceramic articles with complex shape, but the additives are sometimes toxic. Additionally the stable time duration of the slurry is limited. Some other methods, such as with cross-linking agents [23] or exposure to UV irradiation [24], with coordinative chemistry [25], and using agar group as a gelling additive [26], are also used for gel casting.

This method shows advantages for shaping the complex parts compared with dry process. It also has the ability to improve the homogeneity of microstructure and increase the optical property and the strength of the final products due to the elimination of agglomerates by using well dispersed suspensions [27, 28].

### 2.3.2 Sintering technology

Sintering is the most important step of the fabrication process. It gives the high alumina ceramic body to its final properties. During sintering, densification, recrystallization, and grain growth occur in the same temperature range. Therefore, a strict control of the sintering process and the amount of grain growth inhibitors, usually MgO, to the alumina powder is essential in order to achieve a fully dense sintered body with fine-grained microstructure. In the course of sintering the density increases with the logarithm of time ( $\sqrt{t}$ ), and the grain size increases with the one-third power of time ( $t^{1/3}$ ) [29].

The choice of sintering temperature and sintering atmosphere depends on the requirement of final properties. It is well known that the sintering of transparent alumina ceramic (PCA) is carried out in hydrogen or high vacuum atmosphere. In this section, we concentrate the sintering technology for transparent polycrystalline alumina by decreasing grain size to nanometer level.

Pressure-less sintered alumina ceramics have been known for several years with sub-micrometer microstructures with a high mechanical strength when defect-avoiding shaping approaches are used with raw powders of  $\sim 200$  nm particle size [10]. These materials exhibited much finer grain sizes than the most fine-grained alumina ceramics mentioned in earlier studies [30]. However, it was difficult to obtain grain sizes  $< 1 \mu\text{m}$  when their relative density is  $\geq 99.95\%$ . Therefore, this problem was solved by using hot isostatic pressing (HIP)

Hot isostatic pressing have in many cases been found to provide unique solutions for problems related to densification of ceramics. The process utilizes uniform and omni directional pressure at elevated temperature to enhance densification and inter particle bonding. It is thus very versatile process with many advantages. In general, voids, particularly large ones [6], in most materials can be efficiently reduced in size and frequency. The reduced sintering temperature means that grain growth and undesirable reaction can be controlled or avoided. As the result, very high strength and small grain size alumina specimens are obtained by HIP.

#### 2.4 Literature surveys of transparent polycrystalline alumina

Transparent polycrystalline alumina (PCA) made via powder processing has been studied by many researchers depending on its applications. There are two major methods to produce transparent alumina. One is the conversion of the polycrystalline alumina to single-crystal by solid-state crystal synthesis method. On the other hand, by controlling the grain size of alumina ceramic to nanometer level, alumina can be transparent. Fig. 2.4 gives the progress of technology to produce transparent

poly-crystalline alumina from 1960s to 2000s. Following this, we concentrate the development of transparent polycrystalline alumina by controlling alumina grain size to nanometer level.

In 1960s Coble [6,31] initially sintered polycrystalline alumina to translucency, free of light-scattering porosity, with mean grain sizes of  $\sim 50 \mu\text{m}$ . Key technologies included are the use of sub-micrometer alumina powder with a small amount of MgO as a sintering aid and the sintering of the pressed compact in a reducing atmosphere at high temperature of  $>1700^\circ\text{C}$ . There had been subsequent investigations to enhance the optical properties of polycrystalline alumina by doping with other elements; however, the still necessary of high sintering temperatures caused exaggerated grain growth, resulting in relatively low mechanical properties [13, 32, 33].

Peelen and Metselaar [34] (1974) showed that transparent alumina with a much smaller grain size of 1-2  $\mu\text{m}$  could be obtained by a continuous hot-pressing process at  $1400^\circ\text{C}$  under a pressure of 120 MPa in different atmospheres. They made clear that the effective absorption coefficient of pure polycrystalline alumina originated from the scattering caused by the remaining pores and the difference between translucent and transparent alumina could be attributed entirely to the difference in pore-size distribution [35]. The in-line transmission of polycrystalline alumina rose strongly from the ultraviolet to the infrared band.

In 1992, H. Mizuta and K. Oda [36] applied slip casting in combination with hot isostatic pressing (HIP) to obtain high-strength and translucent sintered products with grain size of 2-5  $\mu\text{m}$ . However, the maximum in-line transmittance was 46% at 1 mm sample thickness and no data on the wavelength of light was given for the specimen with larger grain size than 5  $\mu\text{m}$  and also no data for the most fine grained samples. The paper stated that residual porosity strongly affected the optical properties in this sample.



In 2000, Yuji HOTTA [37] demonstrated that translucent alumina ceramics could be successfully produced by slip casting using a gypsum mold, provided that impurities, which penetrated into the green compacts from the gypsum mold, were removed by the washing of HCl aqueous solution from the calcined compacts.  $\text{Al}_2\text{O}_3$  ceramic samples were sintered at  $1350^\circ\text{C}$  for 2 h under vacuum. The relative densities of sintered  $\text{Al}_2\text{O}_3$  ceramic compacts with HCl treatment were slightly higher than those of the untreated samples. Grains in HCl-treated samples grew homogeneously to about  $1\ \mu\text{m}$  in diameter. The sintered  $\text{Al}_2\text{O}_3$  ceramics with HCl treatment were translucent. Transmittance values were measured by spectroscopy, and increased from 0 to 12% as the wavelength increased from 300 to 900 nm.

Dirk Godlinski et al. (2003) [38] investigated the formation of a uniformly packed green body which is necessary preconditioned to obtain a fully dense polycrystalline alumina with submicrometer grains that allows high transparency for visible light. It was shown that transparent alumina could be produced with submicrometer grains by processing commercially available powders in aqueous route followed by sintering at low temperature. Essential issues were provided by the float-packing process, which is based on the controlled stabilization of the powder suspension and a concurrent consolidation step. These processes were regulated in such a way that the setting of the fraction of the finest particles while persisting in the fully stabilized mode, proceeded after the sedimentation of larger particle and agglomerates. Random closed packing was then enabled during slow volatilization of the solvent leading to defect-free green microstructure. After sintering at  $1275^\circ\text{C}$ , the dense unmachined parts exhibited mirror-like surfaces with typical roughness of  $R_a = 10$  nm and transmission properties comparable to commercial coarse-grained alumina products for lamp envelopes.

In 2003, Apezt and Bruggen [8] studied the effect of grain size of alumina on transmittance by using the model based on Rayleigh-Gans-Debye light scattering theory. The model was applicable to any type of optically anisotropic ceramic material if the anisotropy and the grain size were not too large. Fine grain samples were prepared by careful colloidal processing. *RIT* values of various samples with a

thickness of 0.80 mm were measured using a red laser with a wavelength of 645 nm. It was found that the in-line transmittance depended on grain size and on the amount and size distribution of a few pores. The in-line transmittance rapidly increased when grain size decreased to sub-micrometer or nano-meter level. The samples exhibited *RIT* up to 71% at a grain size of 300 nm.

Andreas Kreal and Paul Blank [39] (2003) showed that transparent alumina with grain size of 0.4-0.6  $\mu\text{m}$  and relative density >99.9% with a real in-line transmission of 55%-65% through polished plates, could be obtained by sintering and HIPing at >1100°C under Ar pressure of 200 MPa. The submicrometer microstructure and the optical properties could be retained for use at >1100°C using dopants that shifted the sintering temperature to high values without additional grain growth. The maximum in-line transmittance of  $\sim 60\%$  was attained by the specimen of 0.8 mm thickness with lapped surfaces for  $\lambda = 650 \text{ nm}$ .

In 2004, Y.Y. O and J.B. Koo [9] investigated the effect of grain size on transmittance and mechanical strength of sintered alumina. Green compacts were prepared by slip casting and the compacts were sintered and HIPed in Ar atmosphere at 1300°C and 101 MPa for 6 h. When the average grain size was between 2 and 7  $\mu\text{m}$ , the sintered alumina did not show any transmittance as a result of Mie scattering. The transmittance increased up to a value of 30% when the grain size was  $\geq 7 \mu\text{m}$ . A high transmittance of  $\geq 50\%$  was obtained by reducing the grain size from 2  $\mu\text{m}$  to 0.8  $\mu\text{m}$ .

Time scale	1960	1970	1980	1990	2000
Translucent alumina produced by sintering alumina to full density, it composed of large grain.	[Hatched bar spanning from 1960 to 2000]				
Transparent alumina produced by conversion of the polycrystalline alumina to single-crystal by solid-state crystal synthesis method.					[Hatched bar spanning from approximately 1995 to 2000]
Transparent alumina produced by controlling of grain size to sub-micron or nanometer level.					[Small hatched bar at the end of 2000]

Fig. 2.4 History of the progress of technology to produce transparent polycrystalline alumina from 1960s to 2000s.

## CHAPTER III

### EXPERIMENTAL PROCEDURES

#### 3.1 Raw materials and characterization

##### 3.1.1 Starting raw materials

Materials, purity and manufacturer of starting raw materials are shown in Table 3.1. The composition data for each material were received from the suppliers.

Table 3.1 Raw materials used in this experiment.

Materials	Purity (%)	Manufacturer
Alumina powder (TMDA)	>99.99	Taimei chemical Co.Ltd., Japan
Mg(NO <sub>3</sub> ) <sub>2</sub> ·6H <sub>2</sub> O	≥99	Ajac chemical Co., Ltd.
Agar powder (M7)	≥99	Ina-shokuhin Kogyo Co., Ltd.
Dispersant (NH <sub>4</sub> salt of PMA, Aron, A6114)		Toagousei Co., Ltd., Japan
PVA (MW. 11000-31000)	98.0-98.8	J.T. Baker Inc.

สถาบันวิทยบริการ  
จุฬาลงกรณ์มหาวิทยาลัย

### 3.1.2 Raw material characterization

#### 3.1.2.1 Particle size distribution

Particle size distribution of alumina powder was determined by laser diffraction method (Particle size analyzer, Mastersizer S Ver. 2.18, Malvern Instruments Ltd.). About 1 gram of alumina powder was mixed with 20 cm<sup>3</sup> of 0.2 wt.% NaHMP aqueous solution and the mixture was ultrasonicated for 5 minutes before measurement.

#### 3.1.2.2 Microstructure observation by SEM

TMDA powder was observed using a scanning electron microscope (JEOL: JSM-6400). Alumina powder was dispersed in distilled water using ultrasonic vibration for 5 minutes. The alumina slurry was dropped on a glass slide, dried in air and then gold sputtered before subjected to the microscope.

#### 3.1.2.3 Specific Surface Area

Specific surface area was measured by BET method. The alumina powder was dried in an oven for 24 h. About 0.2 gram of powder was put in a cylinder tube of COULTER SA 3100 surface area and pore size analyzer.

#### 3.1.2.4 Thermal properties of $Mg(NO_3)_2 \cdot 6H_2O_{(s)}$ and agar

In order to study the decomposition temperature of agar powder and thermal change of magnesium (II) nitrate hexahydrate to MgO, thermal analysis instrument (DTG Perkin Elmer) was used from room temperature to 1000°C. About 5 mg of sample was loaded into an alumina crucible. After that, it was heated from 30°C to 1000°C at a heating rate of 20°C/min and held at 1000°C for 5 minutes.

### 3.2 Composition and Preparation of alumina green body.

Alumina powder was mixed with MgO in the form of  $\text{Mg}(\text{NO}_3)_2 \cdot 6(\text{H}_2\text{O})$ . The compositions of mixtures are shown in Table 3.2.

Table 3.2 Compositions of alumina powder with MgO.

Compositions	Alumina (wt.%)	MgO (wt.%)
TR1	100.0	0
TR2	99.99	0.01
TR3	99.97	0.03
TR4	99.95	0.05
TR5	99.90	0.10

#### 3.2.1 Preparation of green body by cold isostatic press method (CIP)

The experimental flow chart is shown in Fig. 3.1. Alumina powder was mixed with MgO (in the form of  $\text{Mg}(\text{NO}_3)_2 \cdot 6\text{H}_2\text{O}$ ) in a polypropylene bottle (250 ml) for 3 hours, using alumina ball as grinding media and 100 grams of ethanol as solvent. The mixture was filtrated and dried. The dried mixture was crushed and passed through a 100 mesh screen. Before forming, sieved powder was well mixed with 1.0 wt.% of polyvinyl alcohol solution (PVA with 11000-31000 MW). Ninety-four grams of alumina powder was mixed with 6 grams of 1.0 wt.% PVA solution in an alumina mortar and the mixture was sieved through a 100 mesh screen. Then it was pressed into pellets of 25 mm in diameter by biaxial hydraulic press with 20 MPa pressure, and followed by cold isostatic press (Dr.CIP, KOBELCO) at the pressure of 200 MPa. The green compacts were dried in an oven at  $105^\circ\text{C}$  for 24 h. Density and microstructures of green bodies were characterized.

The dried bodies were calcined at  $800^\circ\text{C}$  for 2 h with a heating rate of  $5^\circ\text{C}/\text{min}$  in air furnace to remove the organic binder and decompose  $\text{Mg}(\text{NO}_3)_2 \cdot 6\text{H}_2\text{O}$  to MgO. The calcined bodies were sintered in both air atmosphere (Box furnace, Linberg

Asherille, Nc., U.S.A.) and under vacuum (High-multi 500, FVPHP-R-5, Fret-20, Japan) of  $10^{-4}$  torr with a heating rate of  $30^{\circ}\text{C}/\text{min}$  to 1250, 1300, 1350, 1450 and  $1550^{\circ}\text{C}$  with a dwelling time of 2 h. Then the specimens were cooled in the furnace to room temperature followed by hot isostatic pressing (Dr.HIP, KOBELCO) at (A)  $1250^{\circ}\text{C}$  and (B)  $1300^{\circ}\text{C}$  for 2 h under Ar pressure of 150 MPa with a heating rate of  $30^{\circ}\text{C}/\text{min}$ . Density, color, microstructure and transparency of sintered and HIPed specimens were observed and characterized.

The best composition with highest density and highest transmittance was selected for gel casting experiment.

### 3.2.2 Preparation of green body by gel casting method

In this experiment, composition TR3 was selected. The experimental flow chart is shown in Fig. 3.2. Alumina slurries were prepared at a solid loading of 65, 70 and 75 wt.% by ball milling for 16 h in a polypropylene bottle with alumina balls. An ammonium salt of poly(methacrylic) acid (Aron, A6114) was used as deflocculant. The optimum deflocculant for each solid loading was studied. Before mixing with agar solution, alumina slurries were degassed under a vacuum of 30 Pa for 30 min followed by ultrasonificating for 10 minutes.

Agar was used as the gelling additive. The agar solution was prepared by mixing the agar powder with distilled water to total concentration of 2 wt.% and dissolved by heating at  $90^{\circ}\text{C}$ . This solution was maintained at  $45^{\circ}\text{C}$  before adding to the alumina slurries.

The well dispersed alumina slurries were kept at  $45^{\circ}\text{C}$  in a water-bath before mixed with agar solution,. The agar solution was added at this temperature. The total amounts of agar added into the alumina slurry were 0.1, 0.2 and 0.3 wt% on the basis of dry alumina powder. Table 3.3 shows the initial and final solid loading in the slurries for the different agar concentrations. The rheological characteristics of the slurries were measured using viscometer.

The alumina slurries were degassed by ultrasonication at 45°C for 10 min before casting. Then it was poured into a PVC moulds (diameter 28.7 mm x 0.5 mm) on the acrylic plate and cooled down to 10°C for 4 h ( usually 4-8 h) in a refrigerator. After the alumina slurries changed to gel, the cast pellets were dried. They were dried before demoulding in the following two routes: (1) Drying in a closed chamber with about 40 litres of volume at room temperature for >72 h. (2) Drying in an open air at room temperature for 48. After that, they were dried in a convection oven at 105°C for 24 hours. Shape, shrinkage and microstructure of green bodies were observed and characterized after drying in oven.

The dried bodies were calcined at 800°C for 2 h with a heating rate of 5°C/min. in air to remove the organic binder and decompose  $\text{Mg}(\text{NO}_3)_2 \cdot 6\text{H}_2\text{O}$  to  $\text{MgO}$ . Densities of calcined bodies were determined. The calcined bodies were sintered at 1300 and 1350°C for 2 h in air furnace with a heating rate of 30°C/min. The sintered compacts were cooled in the furnace to room temperature, and followed by hot isostatic pressing (HIP) at 1300°C for 2 h under argon pressure of 150 MPa with a heating rate of 30°C/min. Bulk density, microstructure and transparency of sintered specimens were observed and characterized.

Table 3.3 Contents of agar and solid loading of  $\text{Al}_2\text{O}_3$  in the slurries.

Compositions	Initial solid loading (wt.%)	Amount of agar to $\text{Al}_2\text{O}_3$ (wt.%)	Amount of agar to water (wt.%)	Final solid loading (wt.%)
G1	65.0	0.10	0.27	63.0
G2	65.0	0.20	0.51	61.1
G3	65.0	0.30	0.74	59.3
G4	70.0	0.10	0.31	67.7
G5	70.0	0.20	0.58	65.5
G6	70.0	0.30	0.82	63.4
G7	75.0	0.10	0.36	72.3
G8	75.0	0.20	0.66	69.8
G9	75.0	0.30	0.87	67.5

สถาบันวิทยบริการ  
จุฬาลงกรณ์มหาวิทยาลัย



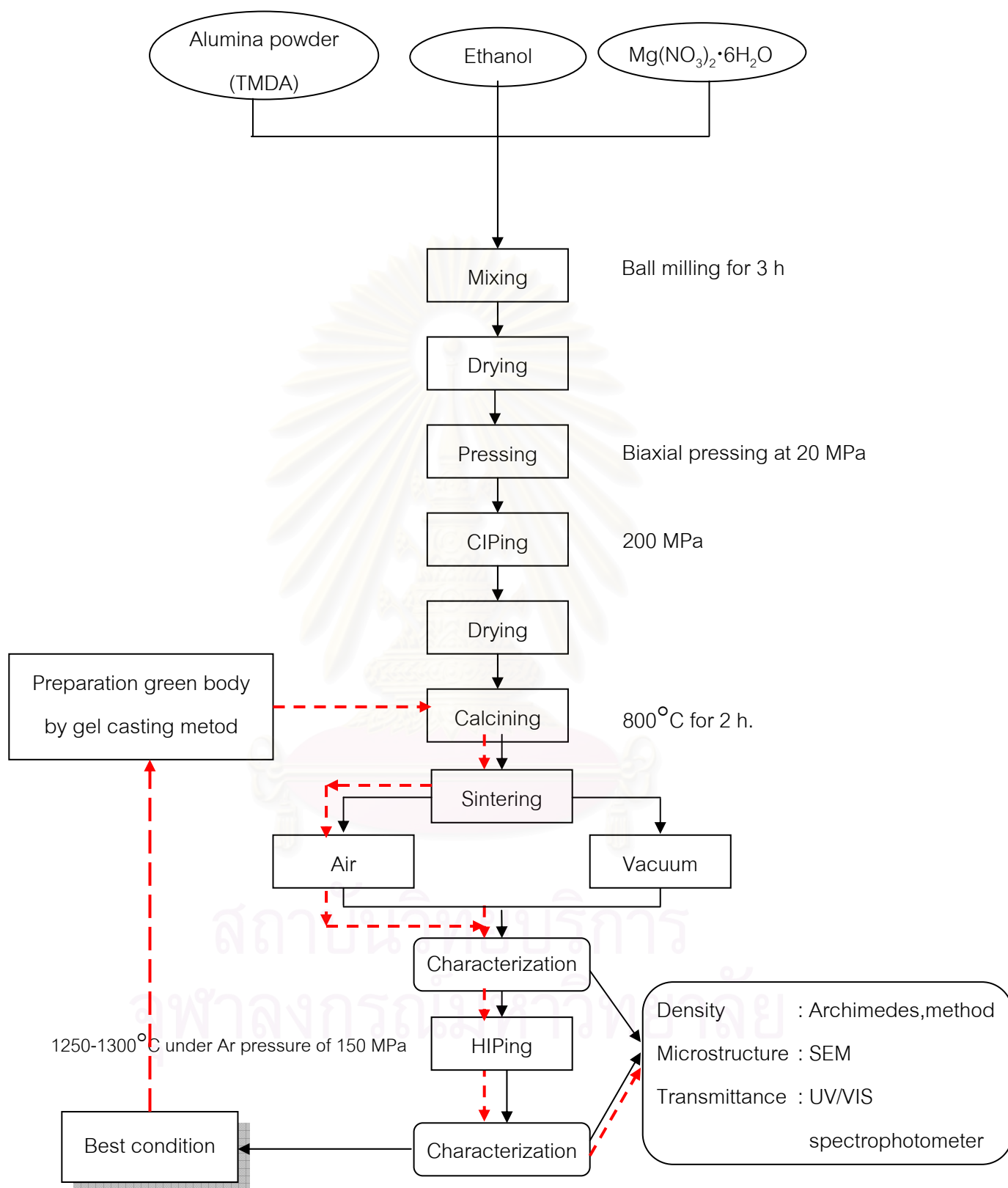


Fig.3.1 Flow chart of green body preparation by cold isostatic pressing process

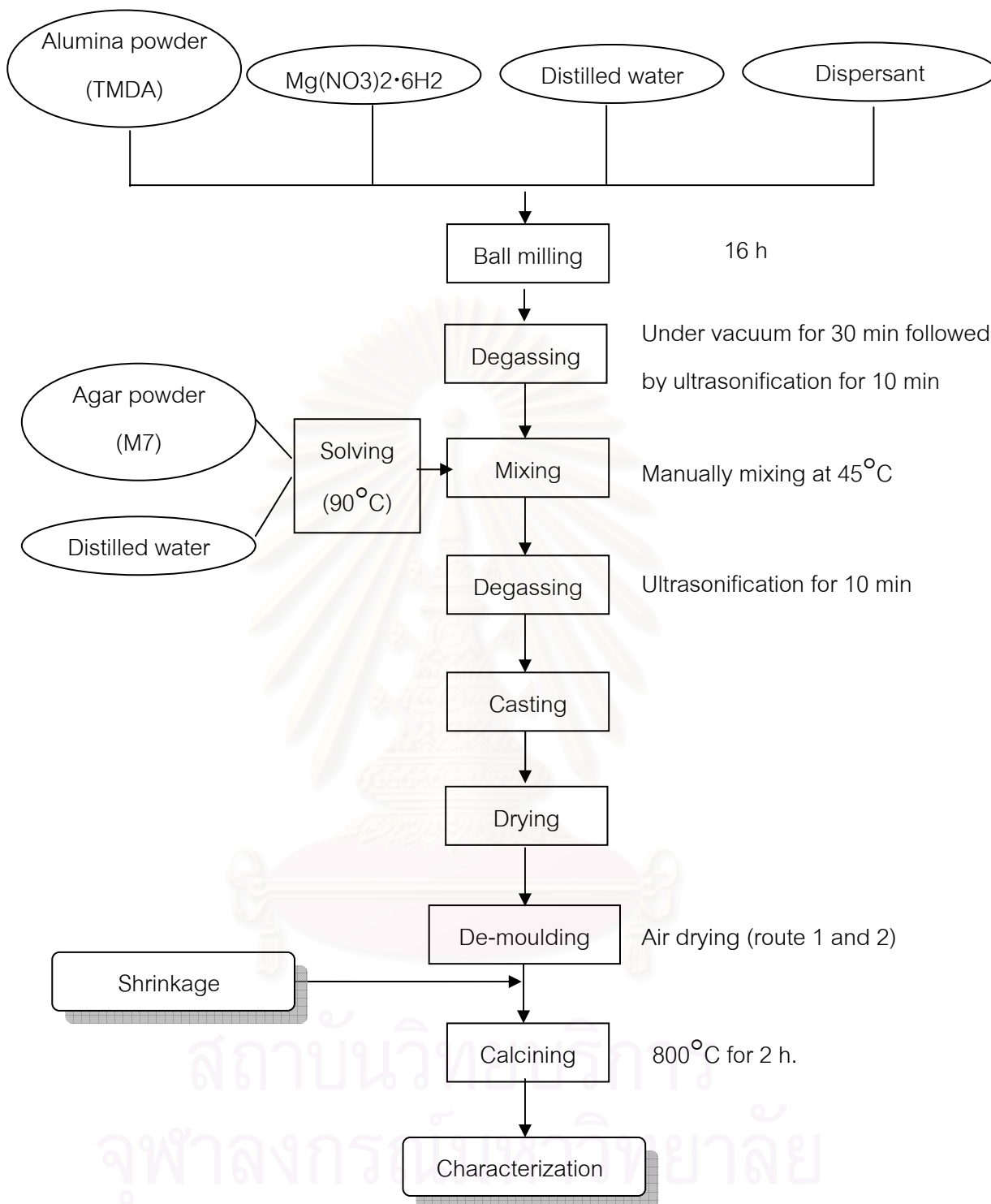


Fig. 3.2 Flow chart of green body preparation by gel casting process

### 3.3 Viscosity of slurry

The rheological properties of alumina slurry and agar solution were measured by rotary rheometer (Brookfield RVDV-E). The alumina slurries and agar solution were prepared separately. The slurry was poured into 250 ml of beaker and then put into a water-bath at a temperature of 45°C, the spindle of viscometer was subjected to the slurry and then viscosity was measured with a constant shear rate of 100 s<sup>-1</sup> for 1 min.

### 3.4 Characterization of green body

#### 3.4.1 Drying shrinkage

The length of green specimen ( $L_g$ ) and length of dried specimen ( $L_d$ ) were measured by vernier caliper. Shrinkage after drying was calculated by the equation (3.1)

$$\% \text{ Linear shrinkage} = \left[ \frac{L_g}{L_g - L_d} \right] \times 100 \quad (3.1)$$

#### 3.4.2 Bulk density

The bulk density of green bodies was calculated by equation (3.2).  $W$  is dry weight of pellet. Diameter ( $D$ ) and thickness ( $T$ ) were measured by vernier caliper. Bulk density of calcined specimen was measured according to Archimedes' method as explained in 3.5.1.

$$\text{Bulk density} = \frac{W}{\pi \left( \frac{D}{2} \right)^2 T} \quad (3.2)$$

### 3.5 Characterization of sintered specimens

#### 3.5.1 Bulk density

The bulk density of sintered specimen was measured according to Archimedes' method (ASTM standard: C830-93) and calculated by equation (3.3).

$$\text{Bulk density} = \frac{W_d}{W_{sat} - W_{sus}} \rho \quad (3.3)$$

Where ( $W_d$ ) is dry weight, ( $W_{sat}$ ) is saturated weight, ( $W_{sus}$ ) is suspended weight and  $\rho$  is water density at measurement temperature referred from reference [40].

#### 3.5.2 SEM Observation

The microstructures of sintered specimens were examined by scanning electron microscope (SEM). The specimens were manually polished with silicon carbide powder, grit No. 2000 and 8000 on a glass plate and finished with 1  $\mu\text{m}$  diamond paste. The polished specimens were thermally etched at the temperature of 50°C lower than the sintering temperature for 1 h. Etched specimens were gold sputtered for 3 min before subjected into microscope. The average grain size were determined by the intercept length method following ASTM standard (E112-96)

### 3.5.3 Transmittance

Transmittance (%T) of sintered specimens was measured using a double beam automatic recording spectrophotometer UV/VIS spectrophotometer. (Perkin Elmer, Lambda 35) The specimens were ground to thickness of 1 and 0.8 mm by BIWAJIMA GIKEN, Japan and polished on both sides by MEITO GIKEN, Japan. The surface roughness ( $R_a$ ) was measured. The data is shown in Appendix H. The transmittance was measured at a wavelength region between 200 to 1100 nanometers.



สถาบันวิทยบริการ  
จุฬาลงกรณ์มหาวิทยาลัย

## CHAPTER IV

### RESULTS AND DISCUSSIONS

#### 4.1 Raw materials characterization

##### 4.1.1 Particle size distribution

Particle size distribution of alumina (TMDA) is shown in Fig 4.1. The size of alumina powder distributed in the range from 100 to 700 nm. The average particle size  $D_{50}$  was 350 nm.

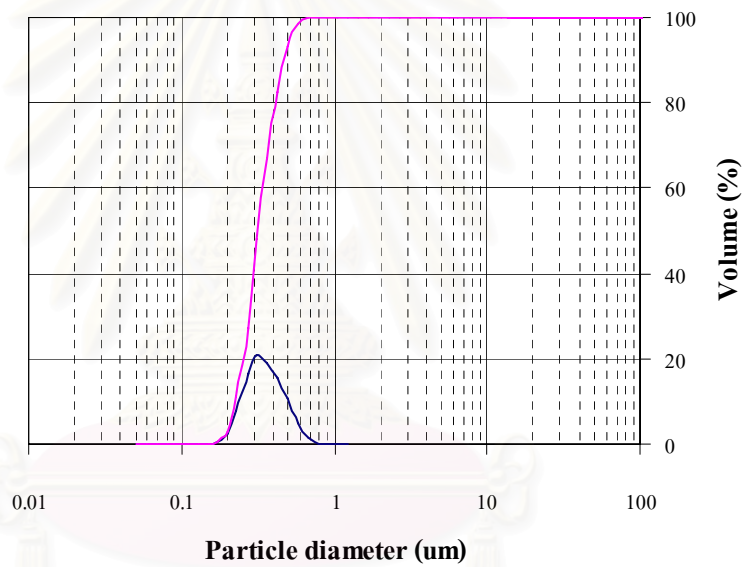


Fig. 4.1 Particle size distribution of TMDA alumina powder.

#### 4.1.2 Shape of alumina powder

SEM micrograph of pure TMDA powder is shown in Fig.4.2. From the SEM micrograph, particle size of alumina powder is smaller than 200 nm and without agglomeration. The particle size, distribution, and state of agglomeration have a strong influence on the microstructure of fired body. In this powder, particles less than 200 nm allow the achievement of high density at low sintering temperature. Homogeneous packing of powder with narrow size distribution generally allows greater control of the microstructure. Free of agglomerates lead to homogeneous packing in green body, which in turn, to homogeneous grain growth during the firing stage. These facts enhance the control of grain size of fired body.

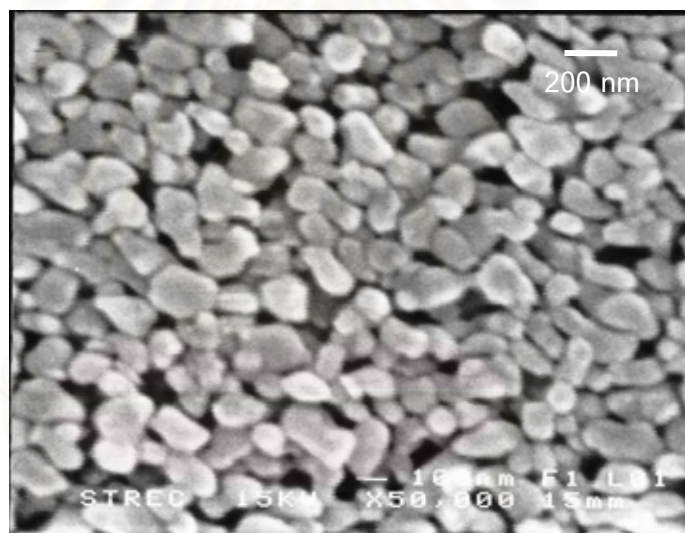


Fig.4.2. SEM micrograph of TMDA powder.

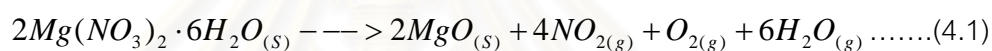
#### 4.1.3 Thermal behavior of $Mg(NO_3)_2 \cdot 6H_2O_{(s)}$ and agar

Thermal behavior of  $Mg(NO_3)_2 \cdot 6H_2O_{(s)}$  and agar were investigated by TGA/DTA as shown in Fig. 4.3 (a) and (b), respectively. The thermal behavior of  $Mg(NO_3)_2 \cdot 6H_2O_{(s)}$  is as follows:

The endothermic reaction at  $\sim 100^\circ\text{C}$  is the removal of free water.

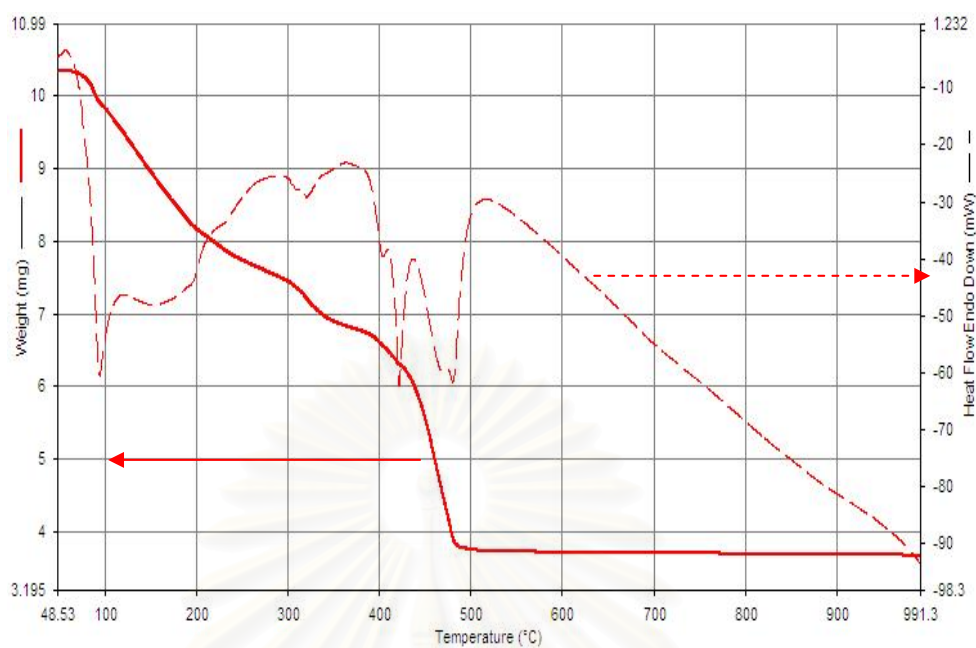
The endothermic reaction at  $420\text{-}430^\circ\text{C}$  is the decomposition of  $H_2O_{(g)}$  from  $Mg(NO_3)_2 \cdot 6H_2O_{(s)}$  crystal.

The endothermic reaction at  $470^\circ\text{C}$  is the decomposition of  $Mg(NO_3)_2$  to MgO and  $\text{NO}_2$ . Therefore,  $Mg(NO_3)_2 \cdot 6H_2O_{(s)}$  finally changes to MgO. The basic reaction is written as:[40]

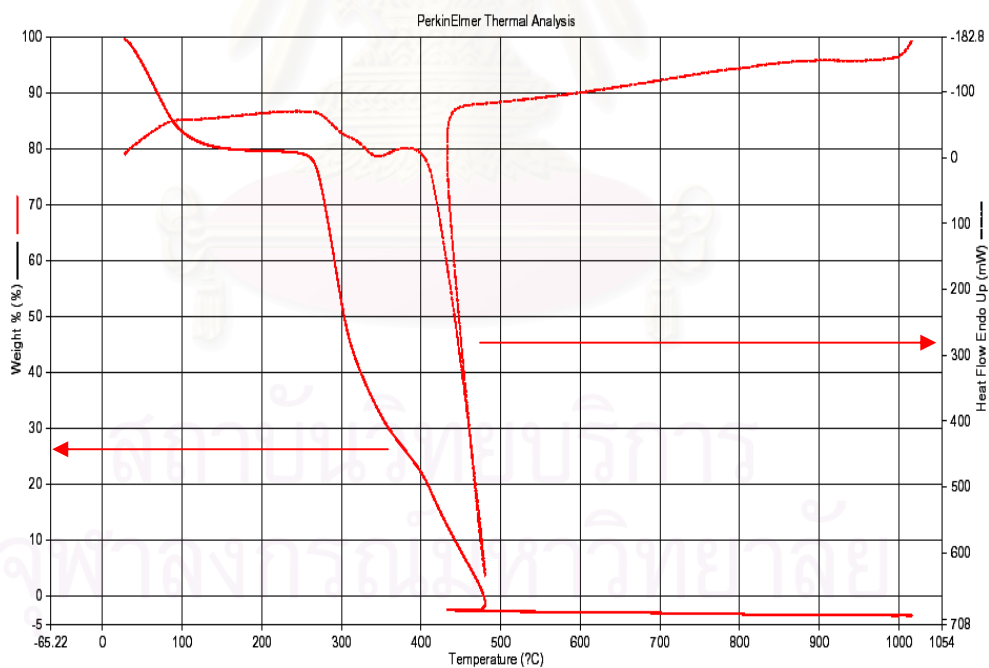


Considering thermal behavior of agar powder, the mass loss occurred from  $250^\circ\text{C}$  and very sharp exothermic reaction occurred at  $400\text{-}450^\circ\text{C}$ . Agar is composed of agarose and agar-pectin. We don't have data how these materials decompose. Moreover, above  $480^\circ\text{C}$ , percent weight loss of agar powder was constant. It means that agar powder completely decomposed when temperature is higher than  $480^\circ\text{C}$ .





(a)



(b)

Fig.4.3 Thermal behavior of (a)  $Mg(NO_3)_2 \cdot 6H_2O(s)$ , and (b) agar powder analyzed by TGA/DTA technique.

## 4.2 Cold press followed by CIP method.

### 4.2.1 Characterization of green body

In order to achieve the submicron or nano-meter level of grain size by pressureless sintering, it is necessary to prepare compact bodies, which lead to high density with good homogeneity. Cold isostatic pressing is one method to attain this characteristic. Fig. 4.4 shows densities of green bodies formed by cold press followed by cold isostatic press method. Density of cold press bodies was about 53% of T.D. and reached to 57% of T.D. when followed by the cold isostatic press at 200 MPa. The fractured surface of green body formed by CIP is shown in Fig. 4.5. It shows good homogeneity without agglomeration.

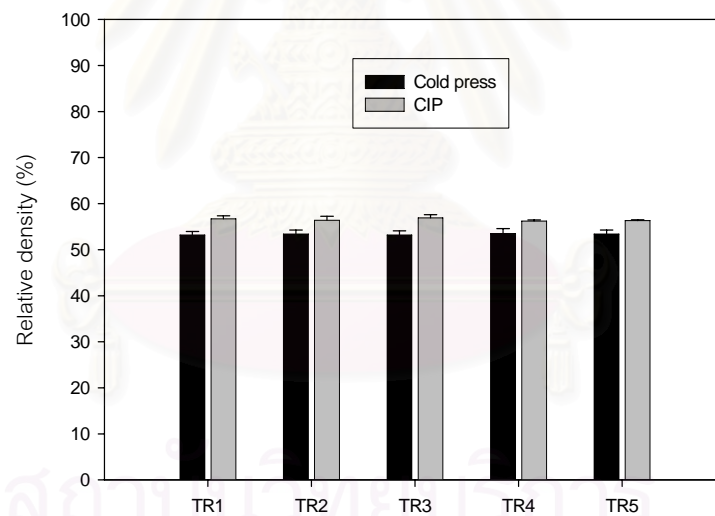


Fig. 4.4 Densities of green bodies formed by cold press and cold isostatic press methods.

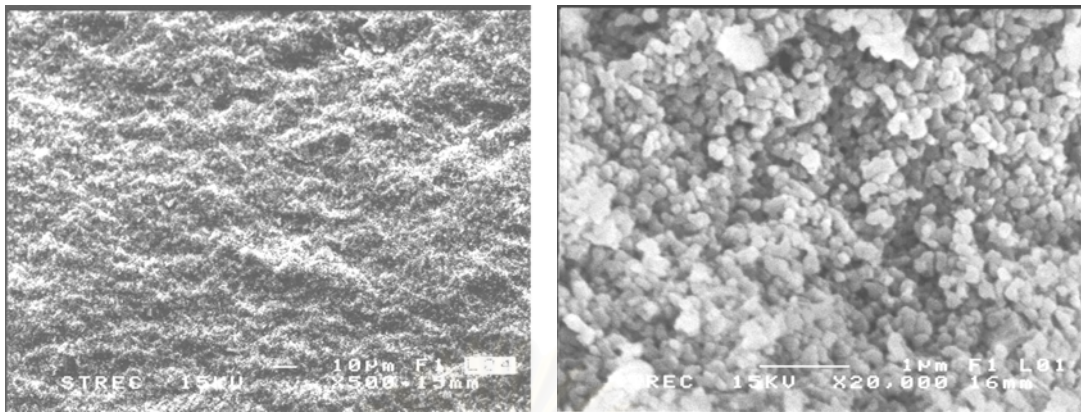


Fig. 4.5 SEM micrograph of fractured surface of green body (TR3) formed by cold isostatic press method.

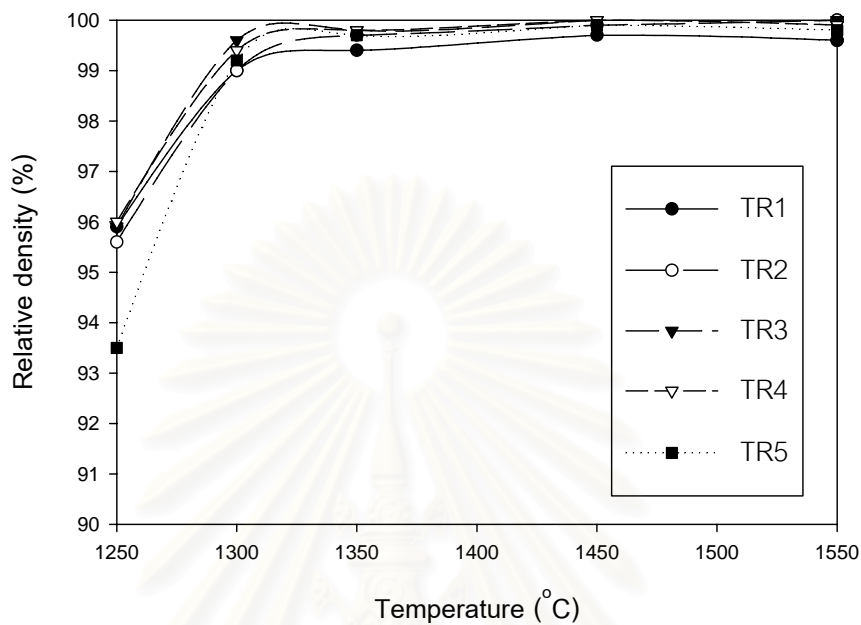
#### 4.2.2 Characterization of sintered specimens

##### 4.2.2.1 Density

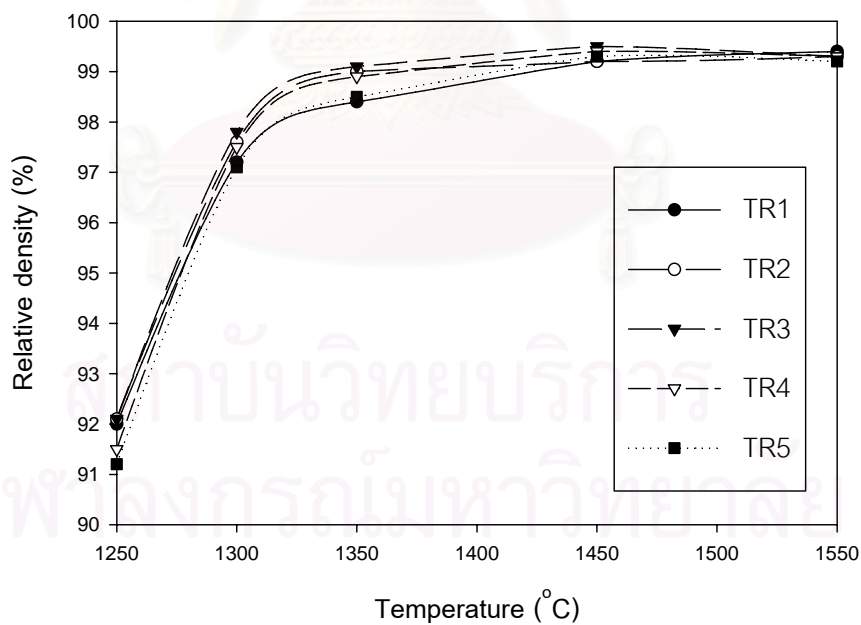
Fig.4.6 shows densities of specimens sintered (a) under vacuum and (b) in air atmosphere at various temperatures. Density of sintered specimens are a strong function of sintering temperature and sintering atmosphere. Increasing the sintering temperature, densities of specimens increased and reached to >99% T.D. at the sintering temperature of 1300°C under vacuum and 1450°C in air atmosphere. The sintering atmosphere plays an important role in achieving a full density. To eliminate the pores it is essential to remove the gas from the pores before they become isolated. Generally, alumina ceramic sintered in air atmosphere will never lead to full density because of N<sub>2</sub> and O<sub>2</sub> gas trapped in the triple junctions between grains. In case of sintering under vacuum atmosphere, no gas molecule was trapped inside the pore because it was evacuated before heating up; therefore, full densities could easily be obtained.

Considering the effect of MgO contents, no any significant difference was found because the nano-size alumina powder was used as raw material which

allowed the achievement of high density at low temperature. Hence, even MgO-free alumina (TR1) could be sintered to nearly full density at low temperature.



(a)



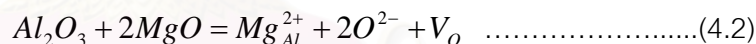
(b)

Fig. 4.6 Relationship between relative density and sintering temperature of alumina compacts formed by CIP and sintered (a) under vacuum and (b) in air atmosphere.

#### 4.2.2.2 Colors






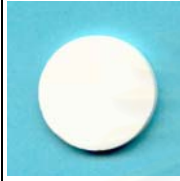


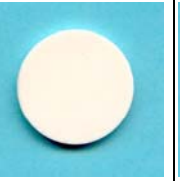
















Colors of specimens sintered under vacuum and in air atmosphere slightly changed from pale-gray to dark-gray and white to yellow, respectively, according to MgO contents and sintering temperature. Table 4.1 and 4.2 shows color of alumina sintered at various temperatures both in air and under vacuum. The change of color due to impurity, additive and sintering atmosphere are common. If magnesia (MgO) was added to alumina the color changed from white to yellow when it was sintered in air, but turned to gray when sintered under vacuum.

Thus, in modern ceramic technology the furnace atmosphere should be carefully controlled. All the coloration effects can be explained by solid state physics. A magnesium ion ( $Mg^{2+}$ ) in the  $Al_2O_3$  lattice causes a free valence. This free valence can interact with electromagnetic radiation. When doping alumina with MgO,  $Al^{3+}$  lattice is replaced by  $Mg^{2+}$  ions (very simplified description). The most common structure imperfections in lattice of alumina such as oxygen vacancies ( $V_o$ ), divalencies ( $V_o - V_o$ ), and also substitutional impurities  $Mg^{2+} \rightarrow Al^{3+}$  [41-43].




























When  $Al_2O_3$  is reduced at high temperature over  $1450^\circ C$  very small amount of oxygen in  $Al_2O_3$  lattice may evaporate and oxygen vacancy will generate.

Table 4.1 Color of specimens sintered in air atmosphere

Temperature (°C)	TR1	TR2	TR3	TR4	TR5
1250					
1300					
1350					
1450					
1550					

สถาบันวิทยบริการ  
จุฬาลงกรณ์มหาวิทยาลัย

Table 4.2 Color of specimens sintered under vacuum.

Temperature (°C)	TR1	TR2	TR3	TR4	TR5
1250					
1300					
1350					
1450					
1550					

สถาบันวิทยบริการ  
จุฬาลงกรณ์มหาวิทยาลัย

#### 4.2.2.3 Microstructure of sintered specimens

Grain size of sintered specimens is a strong function of sintering temperature. Increasing the sintering temperature grain size of specimens increased, as shown in Fig.4.7. Grain sizes of specimens sintered at 1350°C for 2 h both under vacuum and in air atmosphere were less than 1  $\mu\text{m}$ , and grew to larger than 1  $\mu\text{m}$  when sintering temperature increased to 1450 and 1550°C. MgO contents did not affect the grain size of alumina at low sintering temperature (1300-1350°C), as shown in Fig.4.8 (a). When sintering temperature increased to 1450°C, MgO-free alumina (composition TR1) showed larger grain size than those of MgO doped compositions (Fig. 4.8 (b)). The presence of MgO at the grain boundary suppressed grain boundaries migration. Therefore, grain growth rate decreased. Comparing the effect of sintering atmosphere on the grain size of alumina at the same sintering temperature, sintering under vacuum promoted grain growth more than sintering in air atmosphere, as shown in Fig. 4.9.

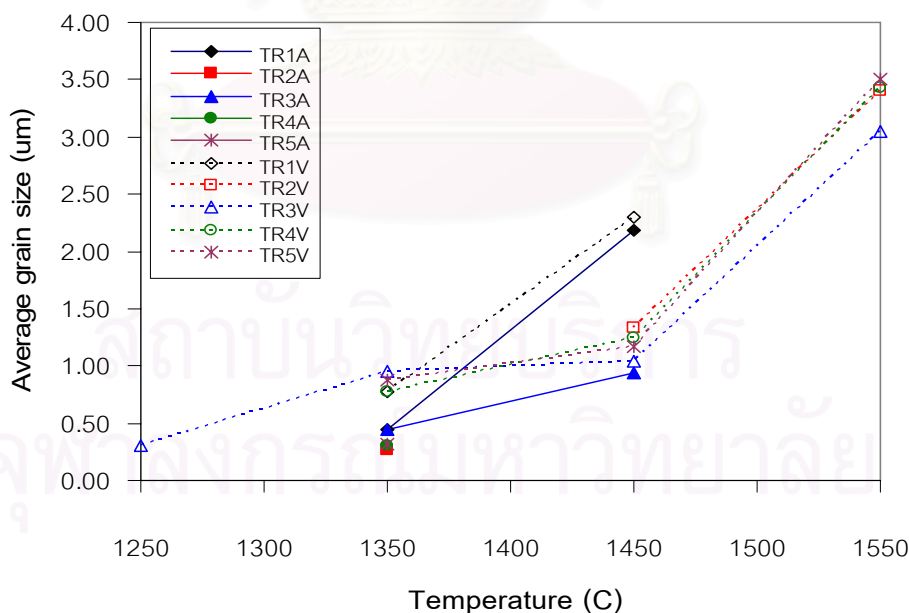
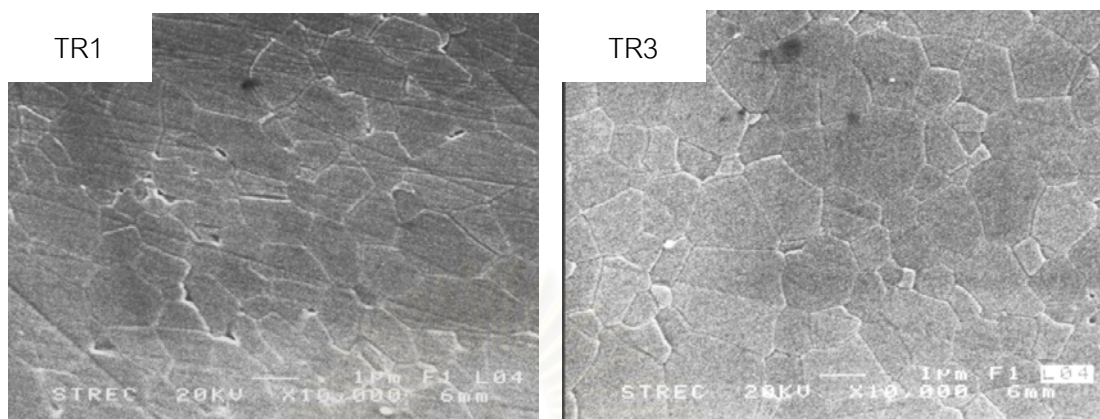
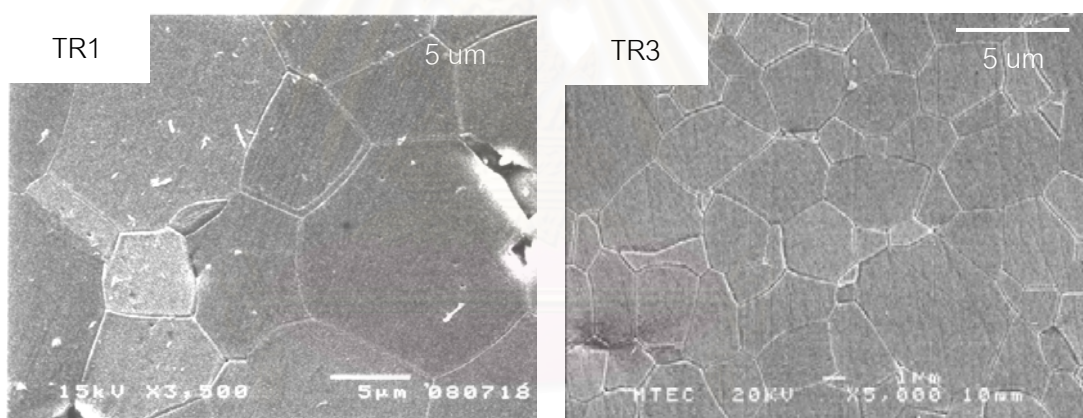


Fig. 4.7 Relationship between average grains size of alumina versus sintering temperature both in air atmosphere and under vacuum.



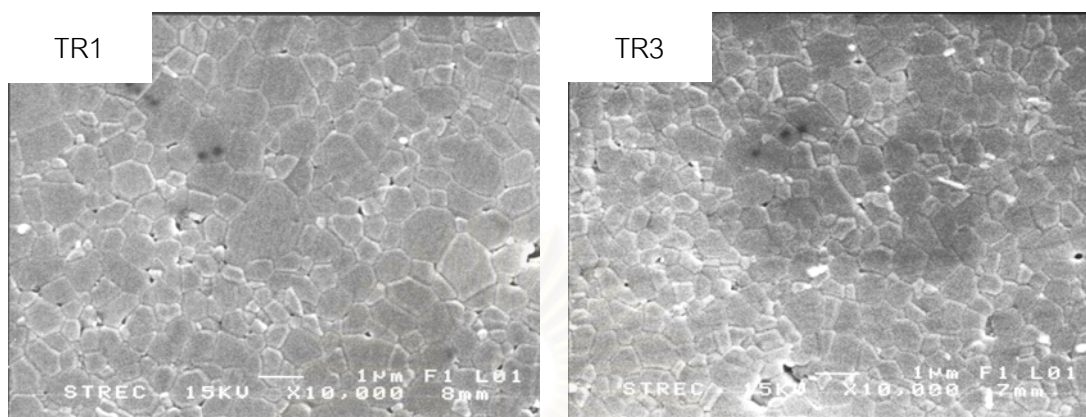


(a)

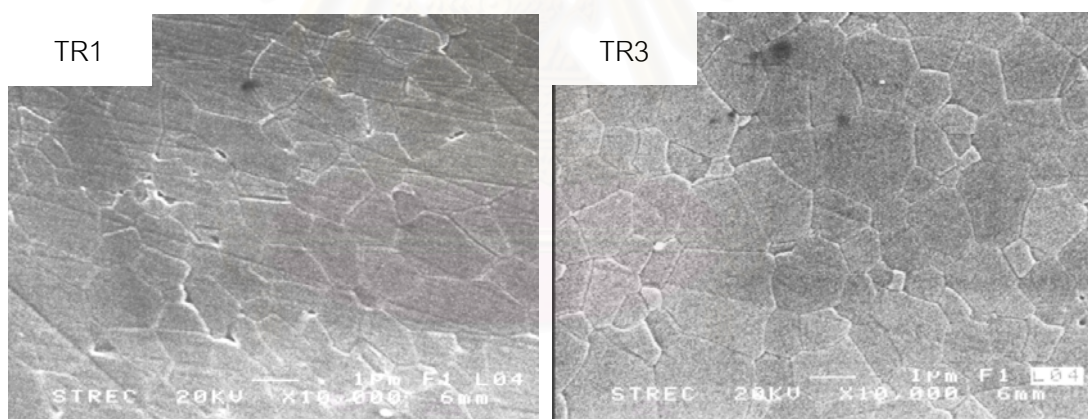


(b)

Fig. 4.8 SEM micrographs of specimens sintered at (a) 1350 and (b) 1550°C for 2 h under vacuum atmosphere.



(a)



(b)

Fig. 4.9 SEM micrographs of specimens sintered at 1350°C for 2 h (a) in air and (b) under vacuum atmosphere.

#### 4.2.2.4 Transparency

Transparency of sintered specimens is a function of sintering temperature, sintering atmosphere and MgO contents. Effects of sintering temperature, sintering atmosphere and MgO contents are discussed.

When composition, sintering rate, sintering atmosphere and sintering time are constant, the transparency of alumina ceramic depended on sintering temperature. Increasing sintering temperature, the transparency increased according to the elimination of the remaining pores.

When TR3 was sintered at  $1550^{\circ}\text{C}$  for 2 h both in air and under vacuum, transparency of sintered specimens was observed. Since transparency is a strong function of sintering atmosphere, the specimen sintered in air atmosphere was opaque. On the other hand, specimen sintered under vacuum was translucent. The sintering atmosphere plays an important role in obtaining a fully dense alumina. To eliminate the pores it is necessary to remove all the gas from the pores before they become isolated. Usually alumina sintered in air atmosphere will never reach full density and is not transparent because of the remaining pores in sintered bodies. When alumina was sintered under vacuum, translucent alumina was obtained. Fig.4.10 shows the transparency of TR3 sintered at  $1550^{\circ}\text{C}$  both in air and under vacuum.

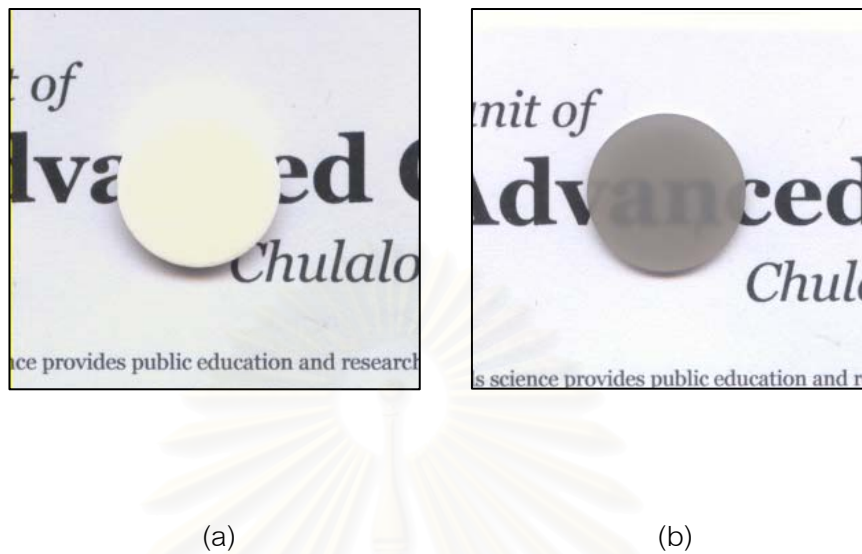


Fig. 4.10 Transparency of TR3 sintered at  $1550^{\circ}\text{C}$  for 2 h (a) in air atmosphere and (b) under vacuum. Both specimens are 1 mm thick and polished on both side.

Fig.4.11 shows the transparency of TR1 and TR3 sintered at  $1550^{\circ}\text{C}$  for 2 h under vacuum. MgO contents had some effects on the transparency of sintered alumina. MgO-free alumina (TR1) was opaque. On the other hand, MgO-doped alumina (TR2, TR3, TR4 and TR5) were translucent. The difference of transparency of TR1 and TR3 was caused by remaining pores remain in the sintered body. In case of TR1, there were many pores trapped inside and at triple junction of grains. By contrast, TR3 had no pores trapped in sintered body. Thus, translucent alumina was obtained only from the sintering under vacuum at  $1450\text{-}1550^{\circ}\text{C}$ .

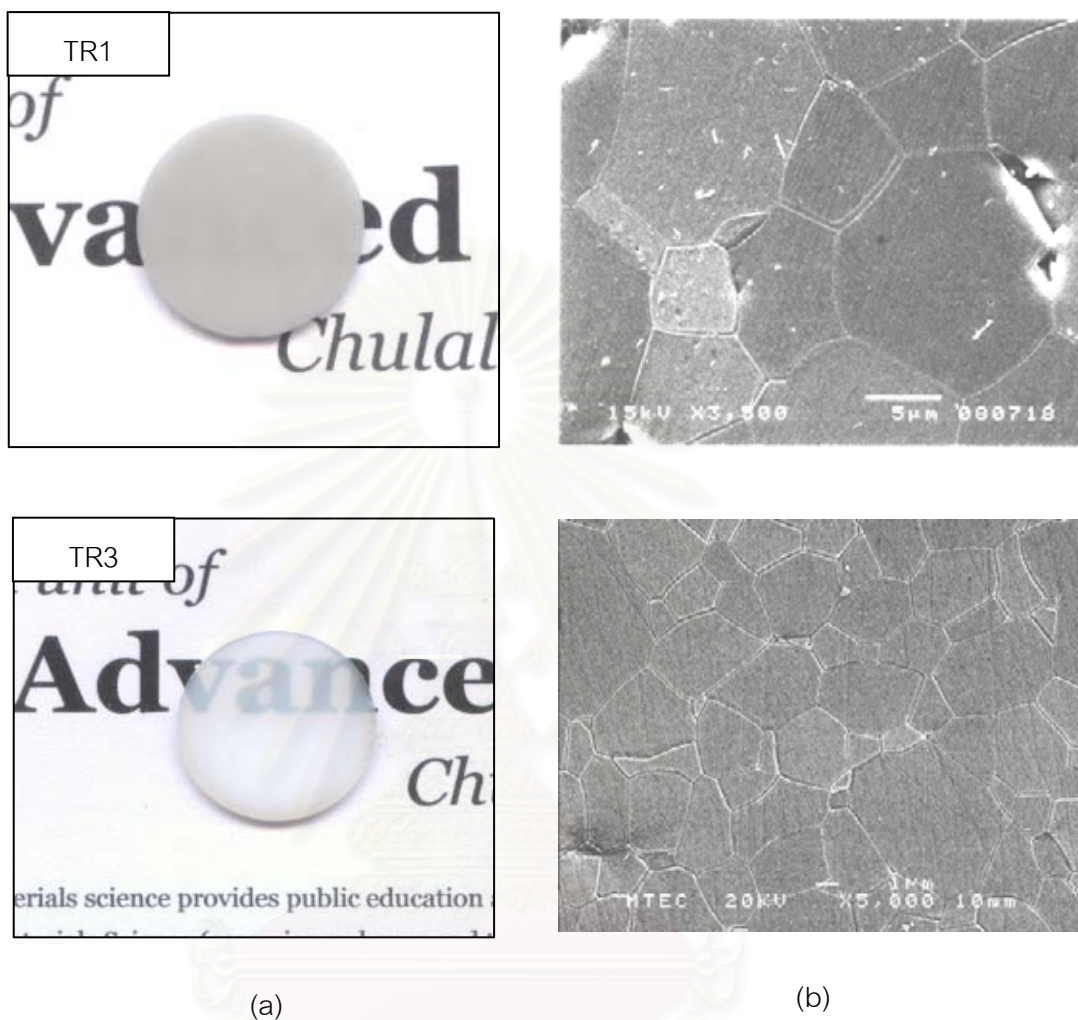


Fig. 4.11 Transparency and microstructure of (a) TR1 and (b) TR3 sintered at 1550°C for 2 h under vacuum.

### 4.2.3 Sinter-HIP

In order to obtain a higher transmittance, density must be increased to full and grain size must decrease to submicron or nanometer level. From the experimental results in the paragraph 4.2.2, we found that, to get the specimen of sub-micrometer or nanometer-size grain, we had to sinter these specimens at the temperature lower than 1350°C. However, it was difficult to obtain full density at this sintering temperature, so we decided to solve the problems by using hot isostatic pressing (HIPing).

In this experiment, cladless Hot Isostatic Pressing or sinter-HIP technology was used. A necessary prerequisite operation prior to the HIP-stage is to sinter the alumina compact to such a high density, >95% of theoretical, that the pores cease to be interconnected to the surface part. The optimum sintering temperature was determined by the preliminary experiment shown in Fig. 4.5 and 4.6.

Specimens sintered at the temperature lower than 1350°C both in air and under vacuum were selected because their densities is high enough for HIPing and their grain sizes were in the sub-micron or nanometer level. The selected specimens for HIPing are shown in Table 4.3. Sintered specimens were put in a graphite crucible, and then Hot Isostatic Pressing (Dr.HIP, KOBELCO) was carried out with Ar gas pressure of 150 MPa at condition (A)1250°C and (B)1300°C for 2 h. Density and transparency were characterized.

Table 4.3 Sintered specimens selected for HIPing.

Temperature (°C)	Composition/ sintering atmosphere									
	TR1V	TR2V	TR3V	TR4V	TR5V	TR1A	TR2A	TR3A	TR4A	TR5A
1250		○	○	○	○					
1300	○	○	○	○	○		○	○	○	○
1350										
1450										
1550			○		○					

Note: A = sintering in air, V = sintering under vacuum, ○ = selected specimens

#### 4.2.3.1 Density of HIPed specimens

Densities of HIPed specimens at conditions A and B are shown in Fig. 4.12 and 4.13, respectively. When the density of pre-sintered specimens exceeds 95% of theoretical, the density of HIPed specimens reached to almost full density. If density of specimen prior to HIPing stage was lower than 95% of theoretical, full density was not obtained after HIPing. It mean that, HIPing is not effective to get full density when open pores still remain in the body. (less than 95% of theoretical).

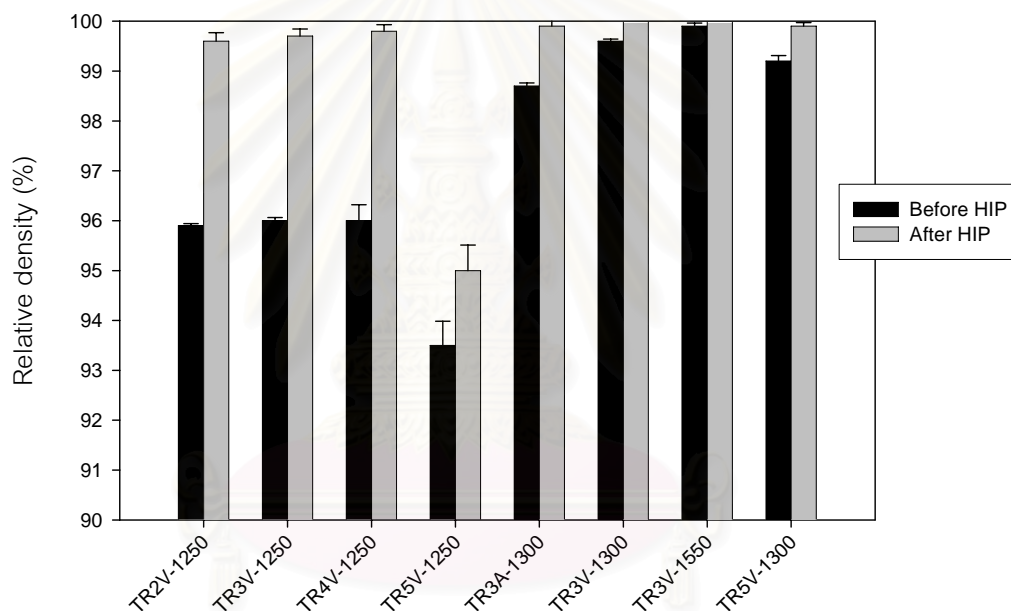


Fig. 4.12 Relative densities of specimens before and after HIPing at condition A, (1250°C, 2 h).

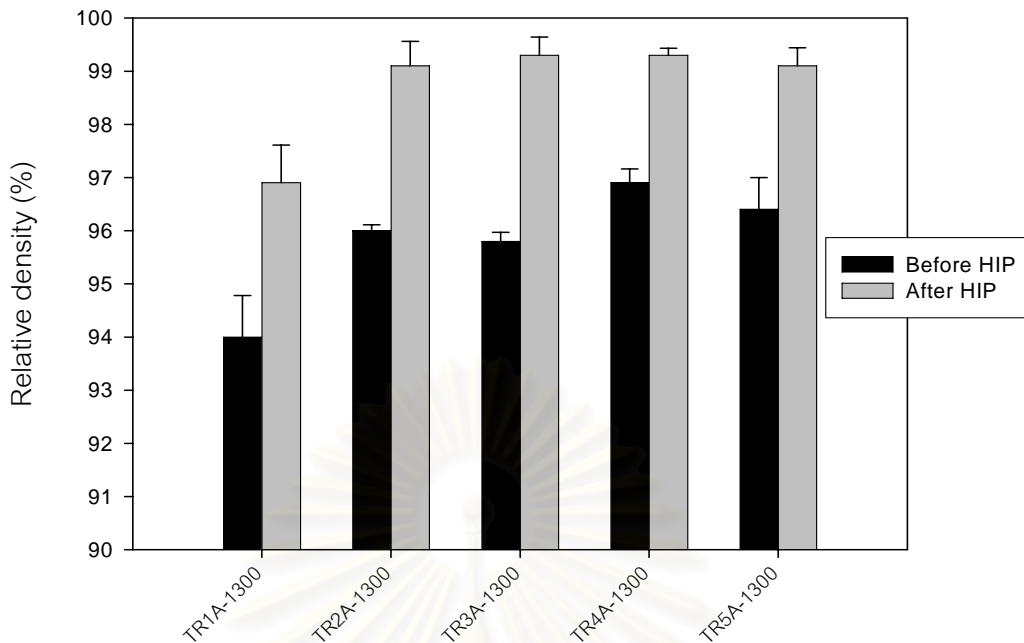








Fig. 4.13 Relative densities of specimens before and after HIPing at condition B (1300°C, 2 h).

#### 4.2.2.2 Color of HIPed specimens

Color of HIPed specimens was strongly influenced by the pre-sintered atmosphere. When alumina pre-sintered in air atmosphere, colors of specimens changed from pale-yellow to transparent after HIPing. By contrast, the colors of alumina pre-sintered under vacuum did not change, but still gray. After heat treatment, the color of TR3V specimen changed from translucent gray to translucent and that of TR3A changed from transparent to yellow. It was summarized in Table 4.5.



Table 4.4 Colors of sintered, HIPed and heat-treated specimens.

Specimens	Color of specimens		
	Sintered specimens	HIPed specimens	Heat-treated specimens
TR3A			
TR3V			

#### 4.2.2.3 Microstructure of HIPed specimens.

Fig.4.14 shows microstructure change of the specimens HIPed at  $1300^{\circ}\text{C}$  for 2 h under Ar pressure of 150 MPa. Before HIPing, the sintered specimen had pores at the grain boundary. After HIPing, it had no pore at the grain boundary. Moreover, grain size of HIPed specimens grew a little larger than the grain size of pre-sintered specimen.

สถาบันวิทยบริการ  
จุฬาลงกรณ์มหาวิทยาลัย

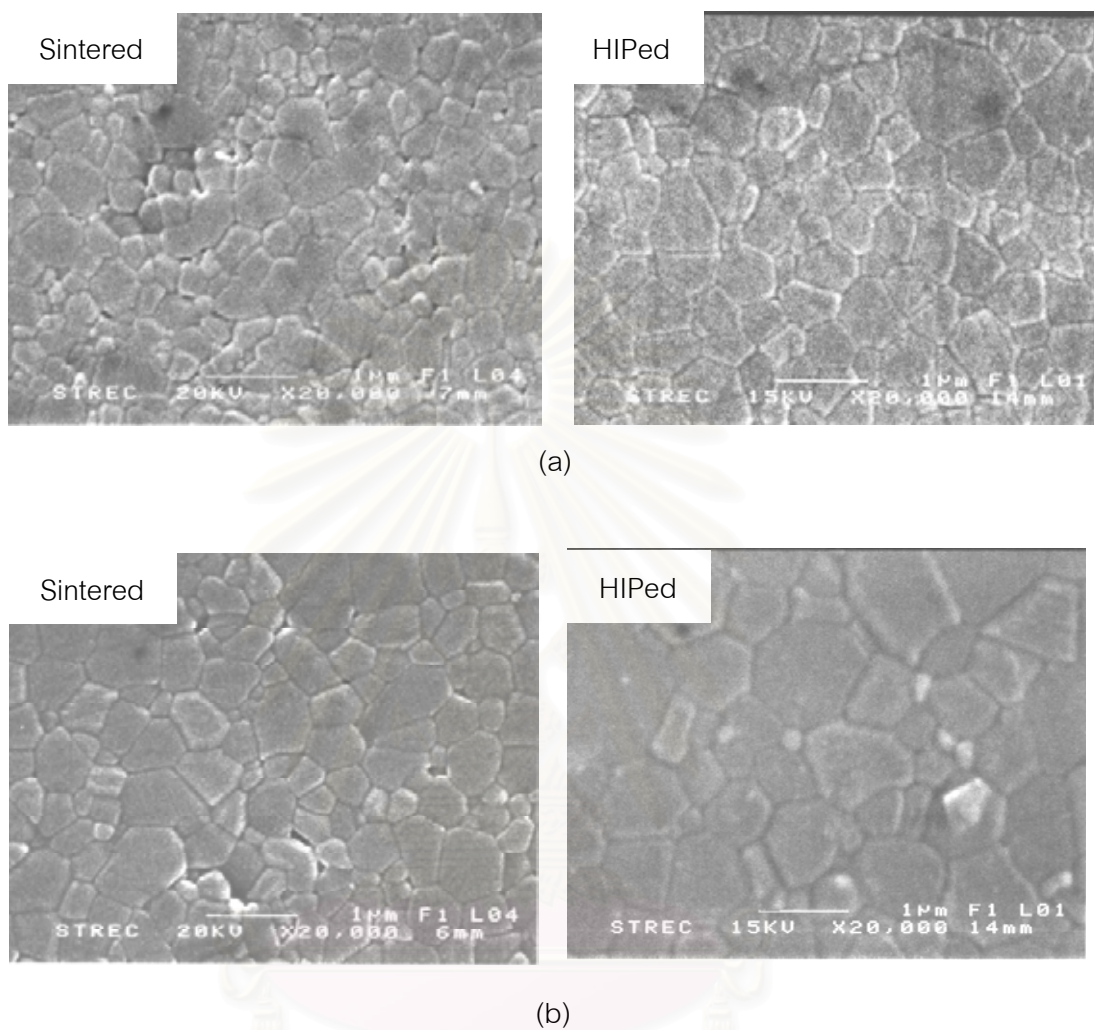


Fig. 4.14 SEM micrograph of TR3 (a) pre-sintered in air and (b) under vacuum followed by HIPing at 1300°C for 2 h under Ar pressure of 150 MPa.

จุฬาลงกรณ์มหาวิทยาลัย

#### 4.2.2.4 Transparency of HIPed specimens

The specimens pre-sintered in air atmosphere at  $1300^{\circ}\text{C}$  for 2 h followed by HIPing at  $1300^{\circ}\text{C}$  for 2 h under Ar pressure of 150 MPa were transparent, as shown in Fig. 4.15 (a). On the other hand, specimens pre-sintered under vacuum followed by HIPing at the same conditions show gray color and transparency was not so good. The difference of transparency of these specimens may be caused by the microstructure difference, as shown in Fig. 4.14. Grain size of specimen pre-sintered in air (TR3A) followed by HIPing is smaller than that of pre-sintered under vacuum (TR3V). It means that, scattering of light at grain boundaries of TR3V is more than that of TR3A. Therefore, TR3A was better in transparency.



Fig. 4.15 Optical micrographs of specimens (a) pre-sintered in air and (b) under vacuum followed by HIPing at  $1300^{\circ}\text{C}$  for 2 h under Ar pressure of 150 MPa. All specimens were ground to 1 mm thick and polished on both side.

Fig 4.16 shows the transmittance (%T) of polished specimens TR2A, TR3A, TR3V, TR4A and TR5A. All specimens were ground to 1 mm thick and polished on both side. The transmittance increased with increasing wavelength. The maximum transmittance of TR2A, TR3A, TR4A, TR5A and TR3V measured at wavelength of 645 nm were 32.8, 40.2, 39.8, 33.4 and 11.4, respectively. Normally the light transmission of transparent poly-crystalline alumina increases with increasing wavelength. When wavelength of light is longer than the grains size of specimen, it passes through specimen without or few scattering at grain boundaries. On the other hand, if wavelength of light is shorter than grains size of specimens, it can not pass through specimen, but refracts, reflects and easily scatters. Therefore, when wavelength becomes shorter, transparency decreases. The increase of the transmission with the decrease in grain size has been recently reported in literature [8].

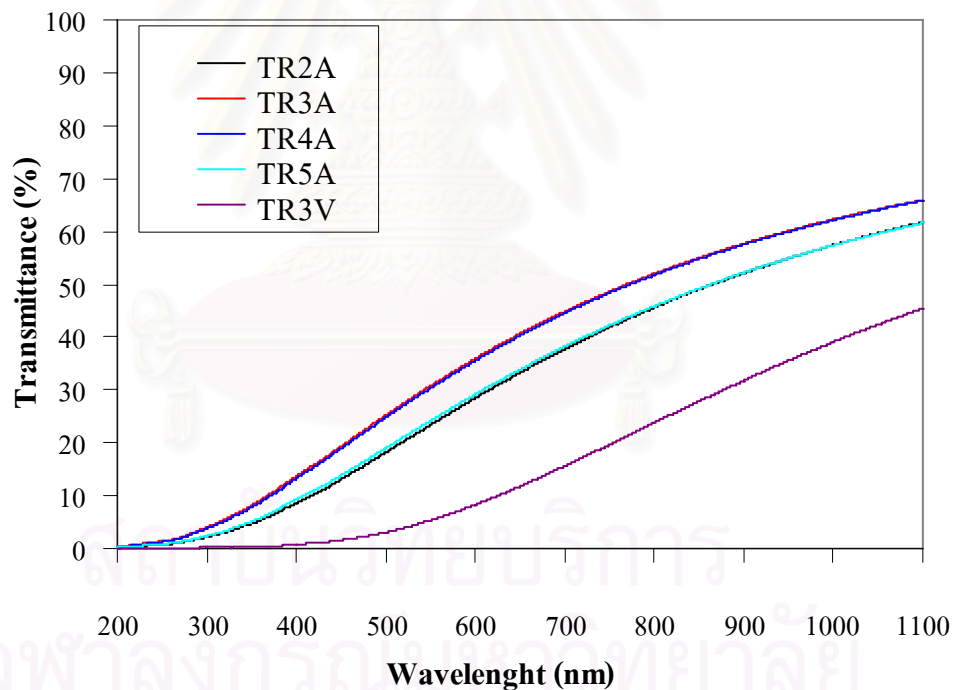


Fig.4.16 Relationship between wavelength and transmittance (%T) of HIPed specimens, the specimens prepared by pre-sintered at 1300°C for 2 h both in (A) air and (V) vacuum followed by HIPing at 1300°C for 2 h under Ar pressure of 150 MPa.

### 4.3 Gel-casting method

#### 4.3.1 Characterization of slurry

Fig. 4.17 shows the relationship between the amount of dispersant (Aron, A6114) and the viscosity of alumina slurries. The optimum amounts of dispersant for 65, 70 and 75 wt.% of pure alumina slurries were 1.0, 1.3 and 1.6 wt.% based on dry solid, respectively. After adding  $Mg(NO_3)_2 \cdot 6H_2O_{(s)}$  to the slurries with minimum viscosity for each solid loading, the viscosity of slurries increased. Then, dispersant was added more. The optimum amount of dispersant for 65, 70 and 75 wt.% alumina slurries increased to 1.3, 1.7 and 1.9 wt.%, respectively. The change of viscosity by adding  $Mg(NO_3)_2 \cdot 6H_2O_{(s)}$  might be caused by the pH shift of alumina slurry, as shown in Fig. 4.18. When  $Mg(NO_3)_2 \cdot 6H_2O_{(s)}$  was added to 70 wt% alumina slurry including 1.3 wt% dispersant, pH decreased from 8.97 to 8.47. On the other hand, viscosity increased from 80 to 300 mPa·S. This mean that, the viscosity of alumina slurry was affected by its pH.

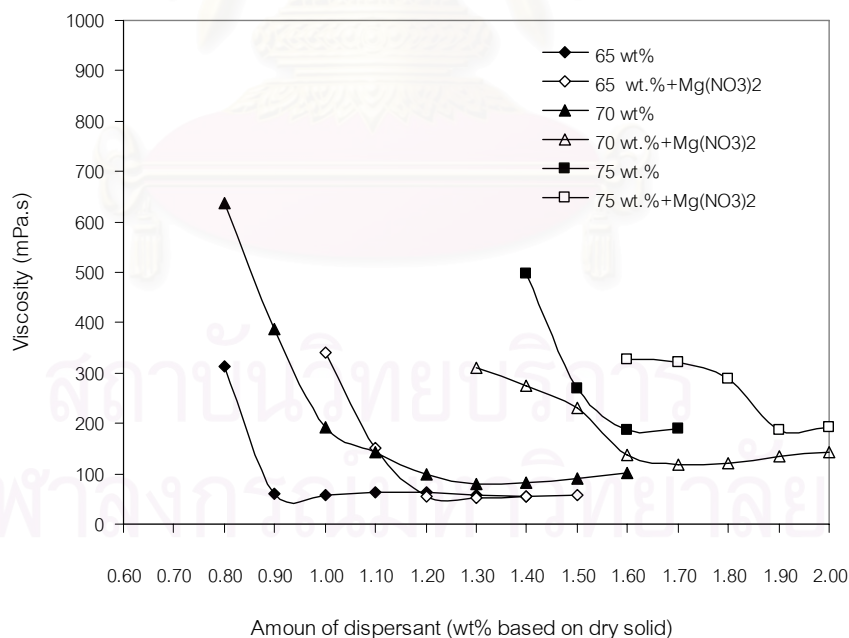


Fig. 4.17 Relationship between viscosity and amount of dispersant (Aron, A6114) in alumina slurries.

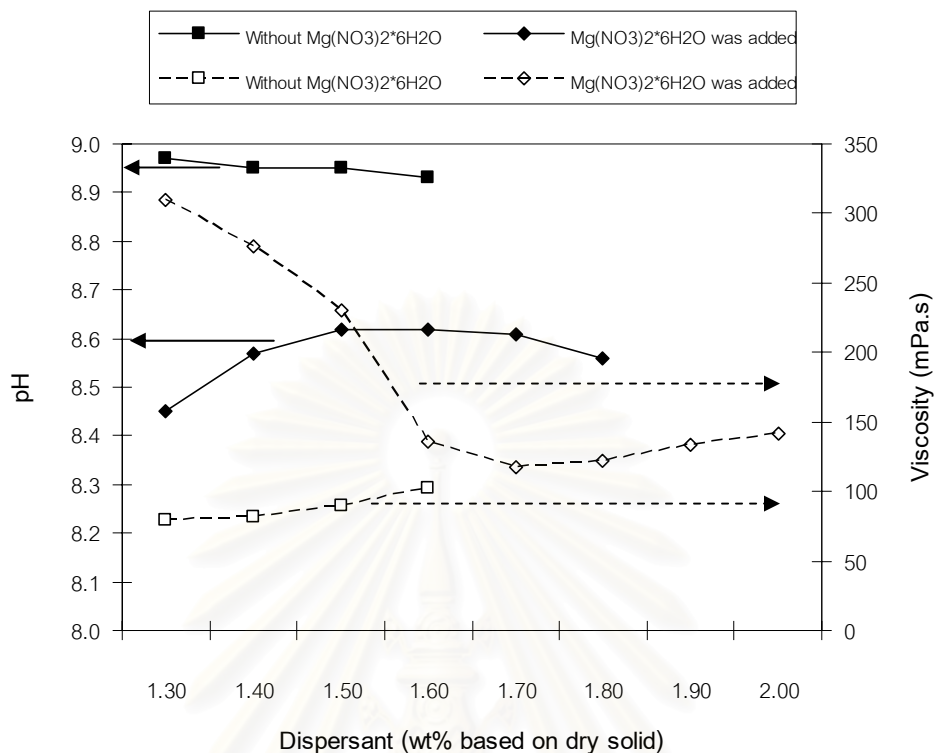


Fig. 4.18 Change of pH and viscosity for 70 wt% alumina slurry with and without  $Mg(NO_3)_2 \cdot 6H_2O$ .

The agar solution was prepared by mixing the agar powder with distilled water to total concentration of 2 wt% and dissolving by heating at 90°C. The evolution of viscosity on cooling was studied in the range of temperatures between 70 and 30°C, as shown in Fig. 4.19. The viscosity of agar solution was low even when the temperature decreased from 70 to 45°C and it abruptly increased > 2000 mPa.s when temperature was further decreased down to 35°C due to hydrogen bonding that led to the development of double helix structure [44]. It was pointed out that at the temperature above 35°C the agar solution did not change to gel, so we could do forming experiment above this temperature range.

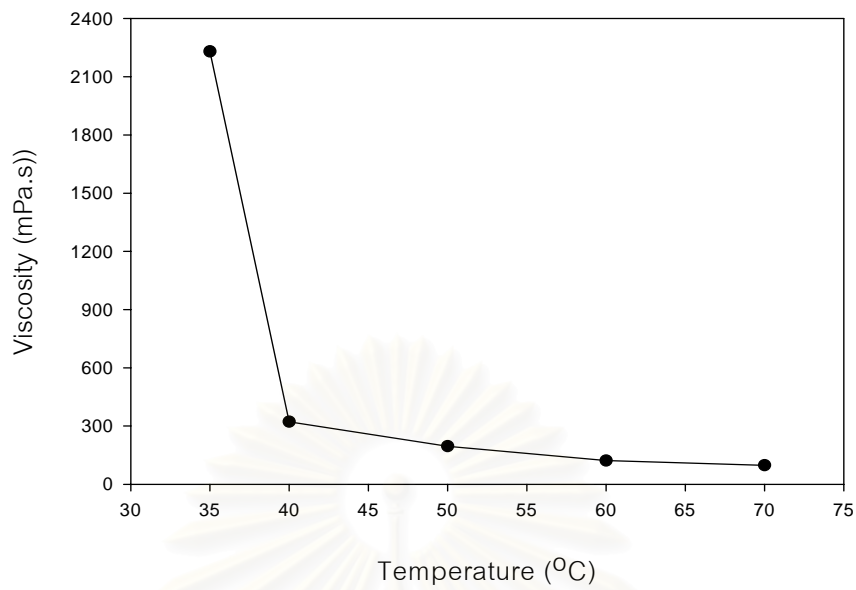


Fig. 4.19 Evolution of viscosity on cooling of 2 wt% agar solution.

Fig. 4.20 shows the relationship between the viscosity values of alumina slurries containing different contents of agar. All the values were measured at the conditions of 45°C and shear rate of 100 s<sup>-1</sup>. In all solid contents, the viscosity increased with increasing agar contents from 0.1 to 0.2 wt.% but slightly decreased with agar contents from 0.2 to 0.3 wt.% except in case of 65 wt% solid loading. This was in agreement with the strong reduction of the solid loading in the final slurries, as can be seen in Table. 3.3. However, all compositions exhibited good fluidity and could be poured into the mold.

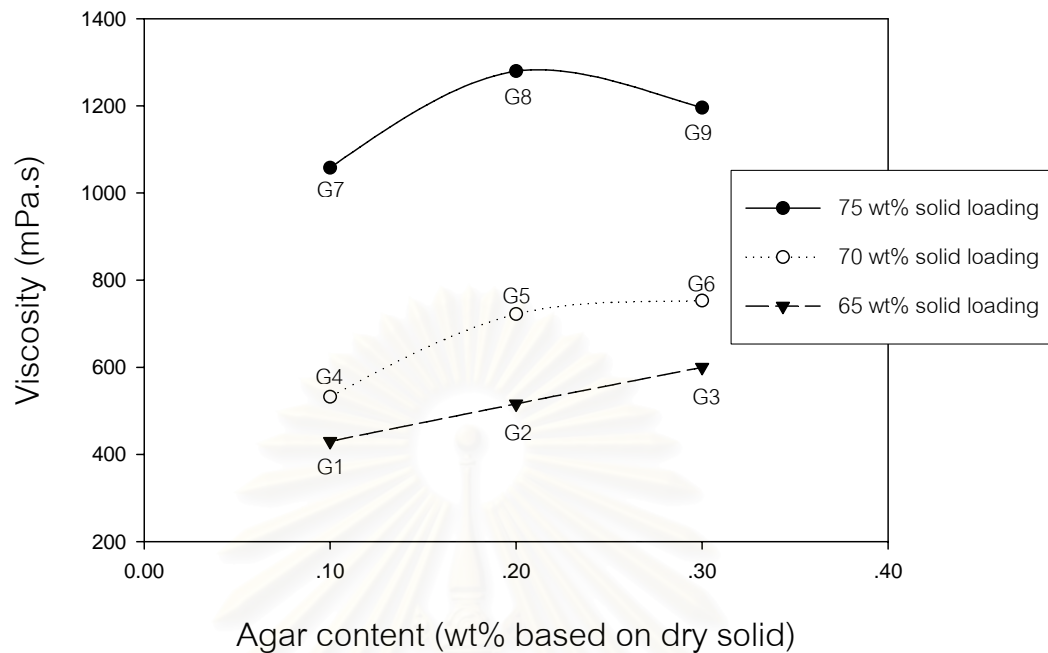


Fig. 4.20 Viscosity of alumina slurries as a function of total content of agar (0.1, 0.2 and 0.3 wt% based on dry solid) at  $100\text{s}^{-1}$  and  $45^{\circ}\text{C}$ .

#### 4.3.2 Characterization of green bodies

The suitable conditions for gel casting depended not only on the viscosity of slurries, but also on the dimension and shape of the obtained bodies. Large deformation was observed for pellets prepared from low solid content slurry, as shown in Fig 4.21. As seen in Fig 4.21, composition G3 showed largest deformation due to the lowest solid content. G2 and G1 were not suitable for gel casting, because they showed deformation and needed longer residence time in the mould. Especially, G1 broke after drying. Another dimension problem was the friction of specimen with the drying support or mould wall which caused nonuniform shrinkage of green bodies.



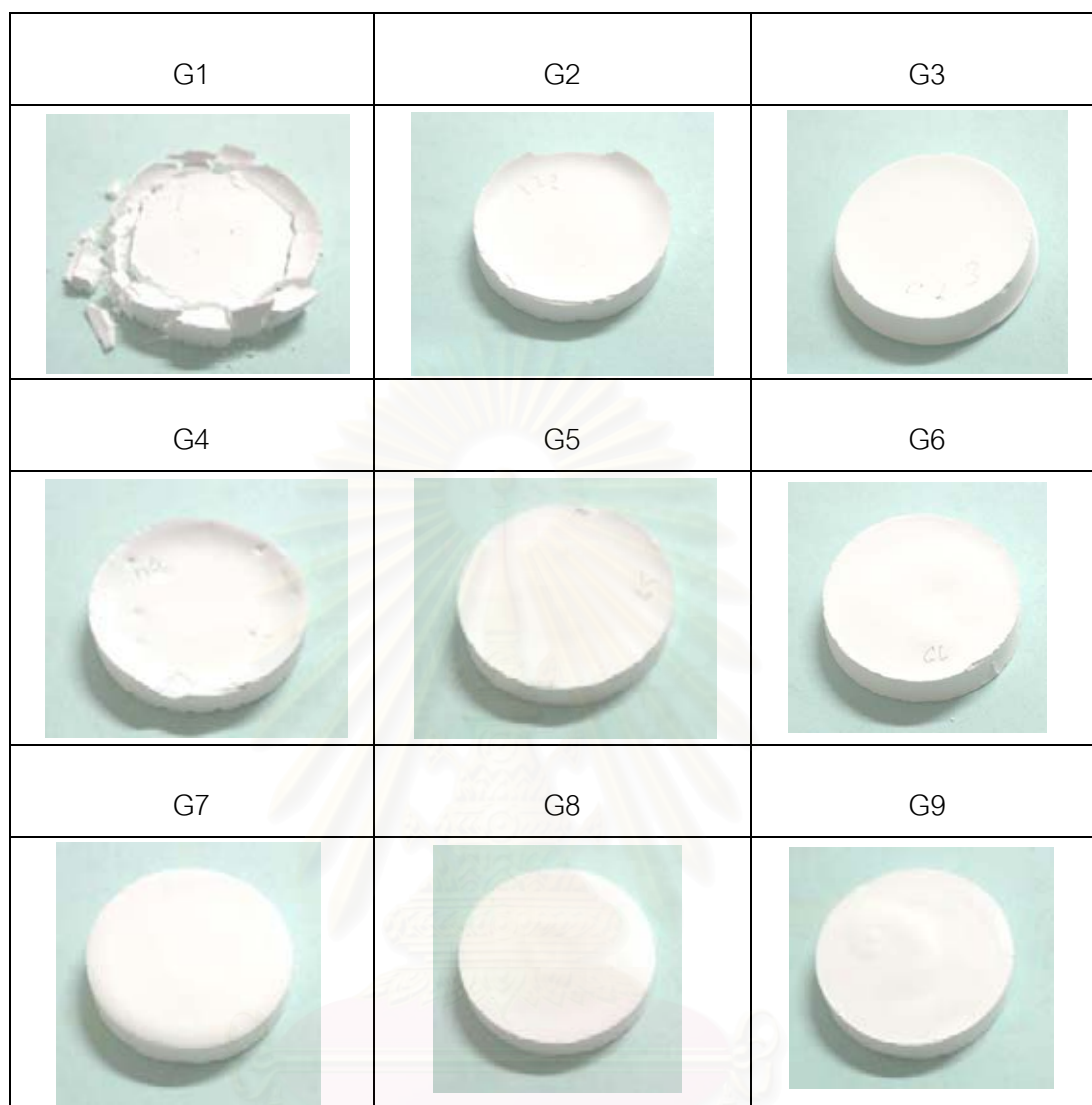


Fig. 4.21 Pictures of green bodies formed by gel casting method.

จุฬาลงกรณ์มหาวิทยาลัย

To control the dimension and shape of dried bodies, the evaporation rate of water from green bodies during drying should be carefully controlled. In this study, the green bodies were dried following the two routes: (1) Drying in closed chamber and (2) Drying in an open air. Fig. 4.22 shows linear shrinkage in diameter of gel-cast bodies after drying at 105°C. The gel-cast bodies had a very large shrinkage after drying, especially when it was stored in the closed chamber (route 1). The difference of shrinkage between route 1 and route 2 specimens was discussed as follows. In route 2, water evaporated quickly. On the other hand, water evaporated slowly in route 1, because moisture increased by the water evaporated. The thickness of specimens dried by route 2 were thinner than that by route 1. Unfortunately the weights of specimen after demoulding and before drying in an oven were not measured. However, water was almost evaporated when specimen was demoulded. Therefore, the large shrinkage of route 1 specimen came from uniform drying. On the other hand, route 2 specimen shrank much in the direction of thickness before demoulding. Hence, the shrinkage was not uniform in the specimen dried by route 2, and resulted in lower shrinkage in diameter.

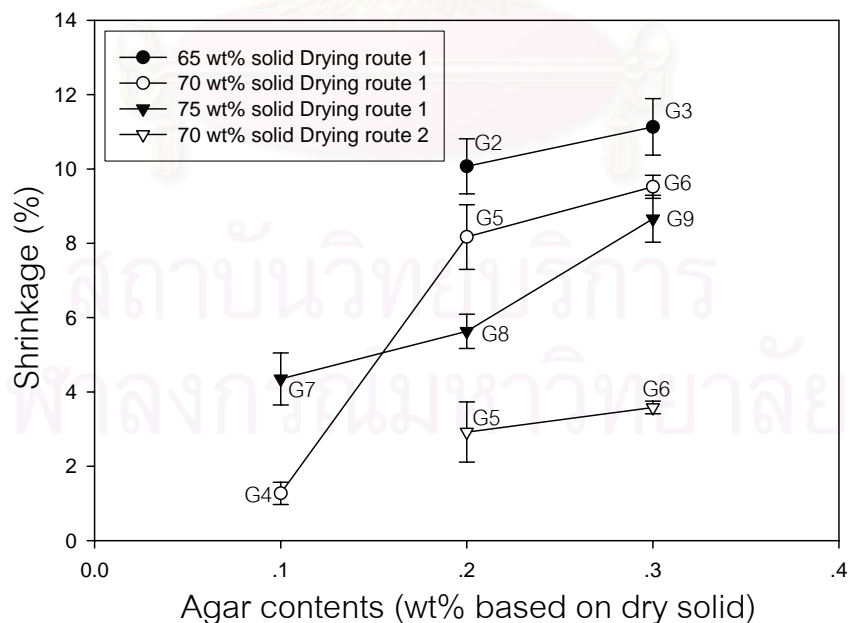


Fig. 4.22 Shrinkage of gel-cast bodies after drying at 105°C.

Density of dried bodies increased with increasing alumina contents as shown in Fig. 4.23 . On the other hand, in all cases the density tended to decrease when total concentration of agar increased. From these result, G7 had highest green density due to highest solid content. Considering effect of drying conditions, there was no significant difference in dry density even when drying method was different. However, drying route 1 exhibited better shape according to the uniformity of shrinkage direction, as shown in Fig 4.24.

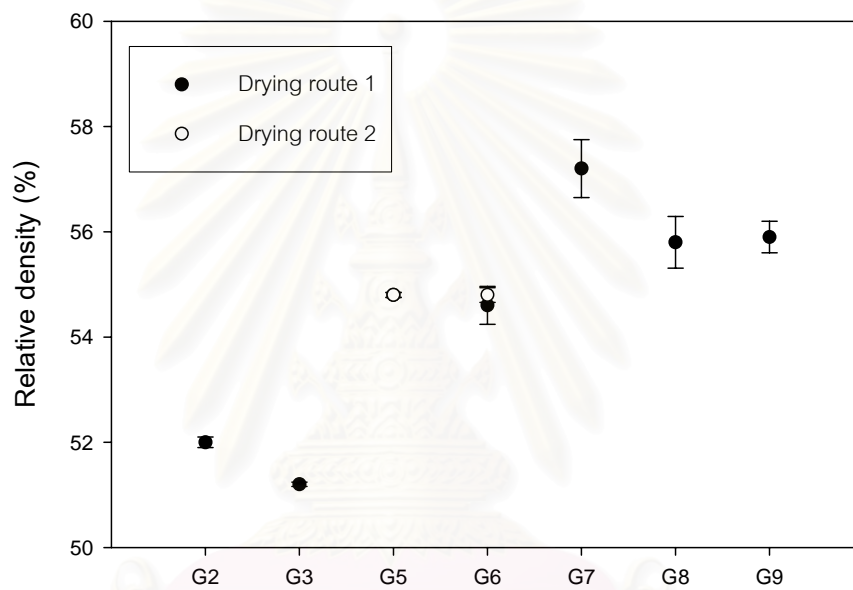


Fig. 4.23 Density of gel-cast bodies of composition G2-G9 dried in route 1 and 2.

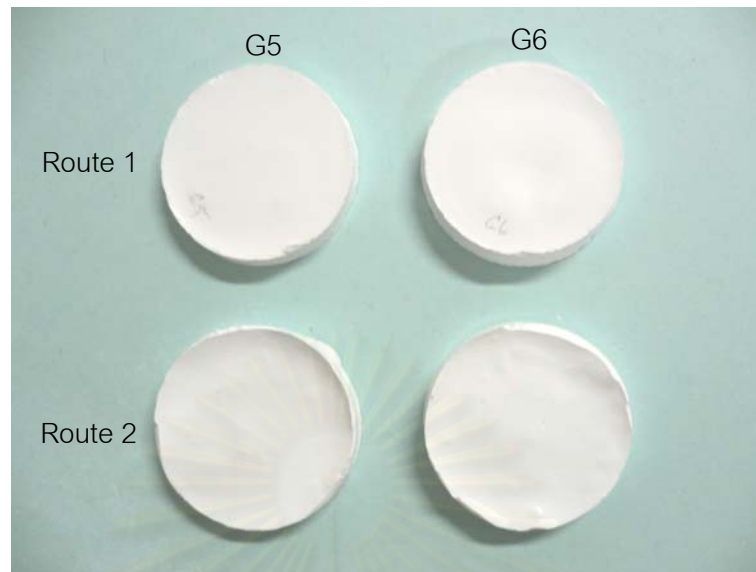


Fig. 4.24 Pictures of gel-cast bodies dried in route 1 and 2.

Fig. 4.25 shows SEM of fractured surface of gel-cast bodies prepared by composition G7, G8 and G9. The fractured surface of all gel-cast bodies were rough which has related to the amount of agar. The roughness increased sharply with increasing the content of agar. Large pore was not found in these bodies. Considering larger magnification (X20000), all specimens exhibited good particle packing. Furthermore, agglomeration was not found in these bodies.

สถาบันวิทยบริการ  
จุฬาลงกรณ์มหาวิทยาลัย

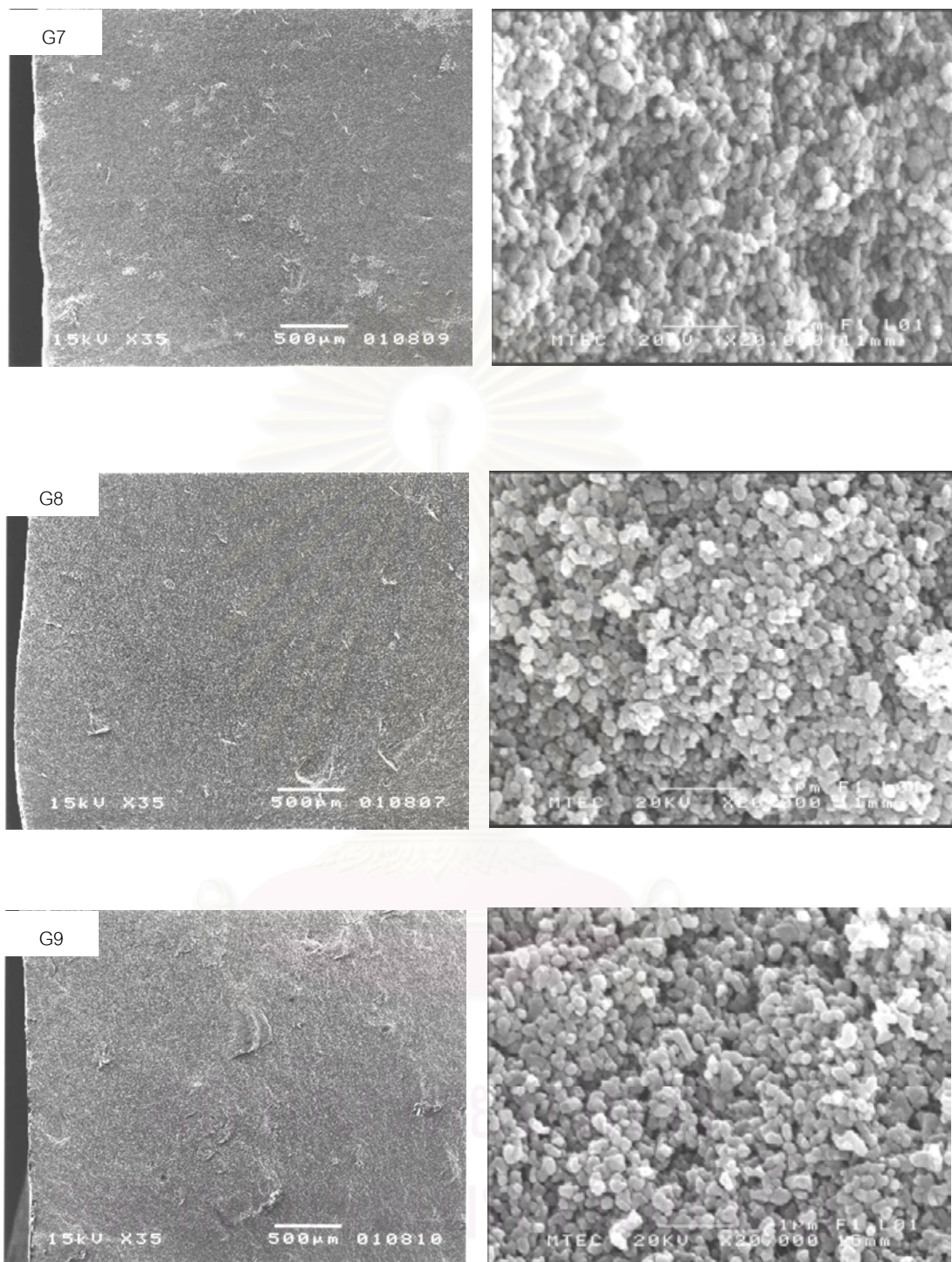


Fig. 4.25 SEM micrographs of fractured surface of green body formed by gel-casting method.

#### 4.3.3 Characterization of sintered specimens.

Fig. 4.26 shows the density of selected specimens sintered at 1300 and 1350°C. Only G7 could be sintered to the condition of closed porosity (>95 % TD.) at 1300°C. When the temperature was increased to 1350°C, the densities of all compositions reached to >95 % TD. However, lower sintering temperature was desirable to suppress the grain growth, so G7 sintered at 1300°C was selected for HIPing.

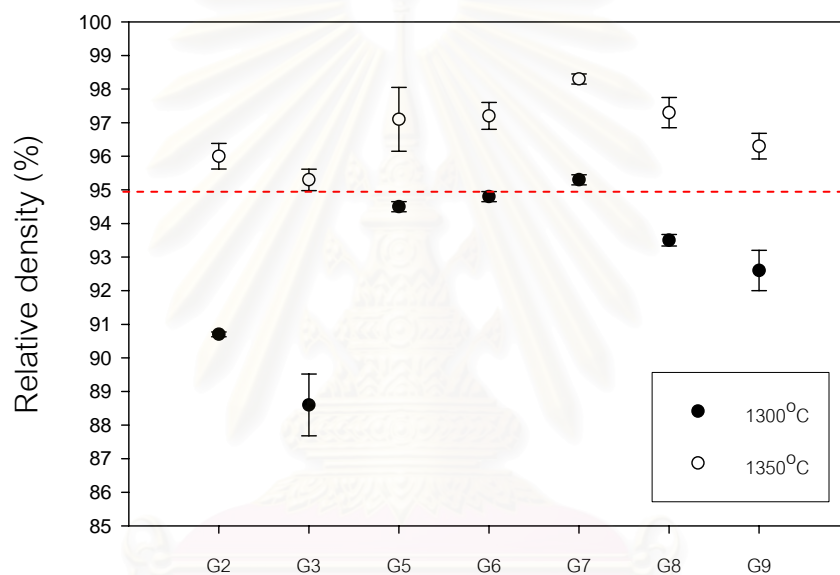


Fig. 4.26 Densities of sintered specimens formed by gelcasting method.

#### 4.3.4 Sinter-HIP

Sintered specimens were put in a graphite crucible, and then hot isostatic pressed under Ar gas pressure of 150 MPa at 1300°C for 2 h. After HIPing, density reached to 100% of TD, grain size increased from 0.34 to 0.56  $\mu\text{m}$ , as shown in Fig. 4.27 .

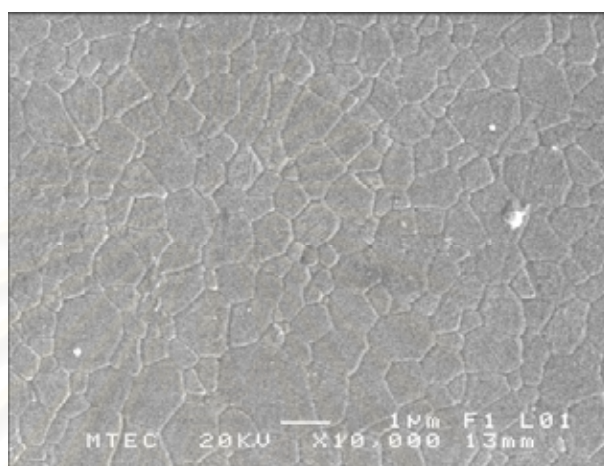
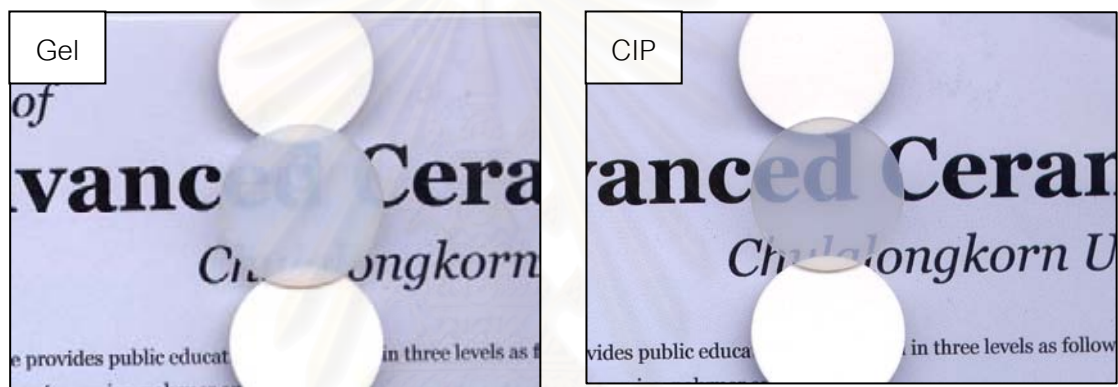
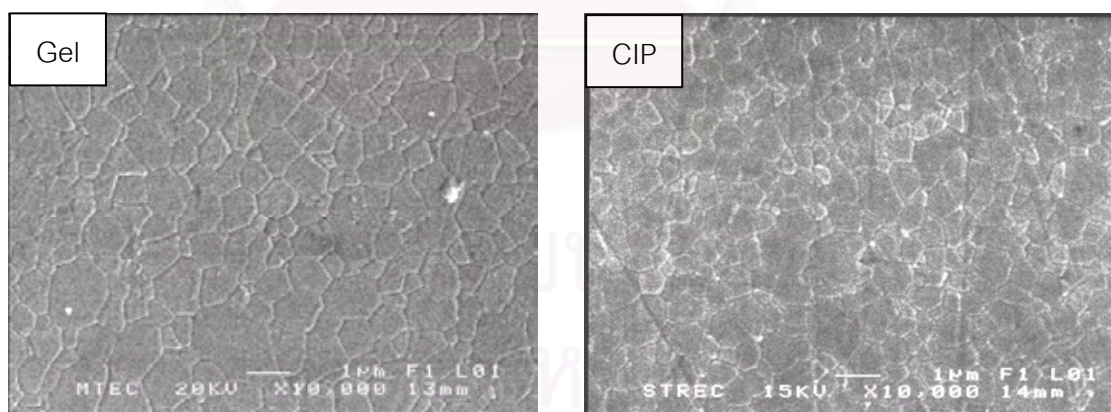


Fig. 4.27 SEM micrograph of G7 pre-sintered at 1300°C for 2 h in air atmosphere followed by HIPing at condition B. (1300°C for 2 h)

Fig. 4.28 (a) shows the transparency of HIPed specimens formed by gel-casting and CIP methods. After HIPing, the gel-cast body was translucent. On the other hand, CIP body was transparent. The transmittance increased with increasing wavelength, as shown on Fig. 4.29. The maximum transmittance of gel-cast and CIP bodies measured at the wavelength of 645 nm were 16.9 and 36.5%, respectively. The difference of transparency and transmittance between the two sintered bodies might be caused by the difference of grain size and distribution of grains, as shown in Fig. 4.28 (b). The average grain size of gel-cast body was  $0.56 \mu\text{m}$  while that of CIP body was  $0.42 \mu\text{m}$ .



(a)



(b)

Fig.4.28. Optical micrographs and microstructures of HIPed specimens formed by gel casting and CIP methods. (the thickness were 0.8 mm.) The distance between disc and printed paper was 1 cm.



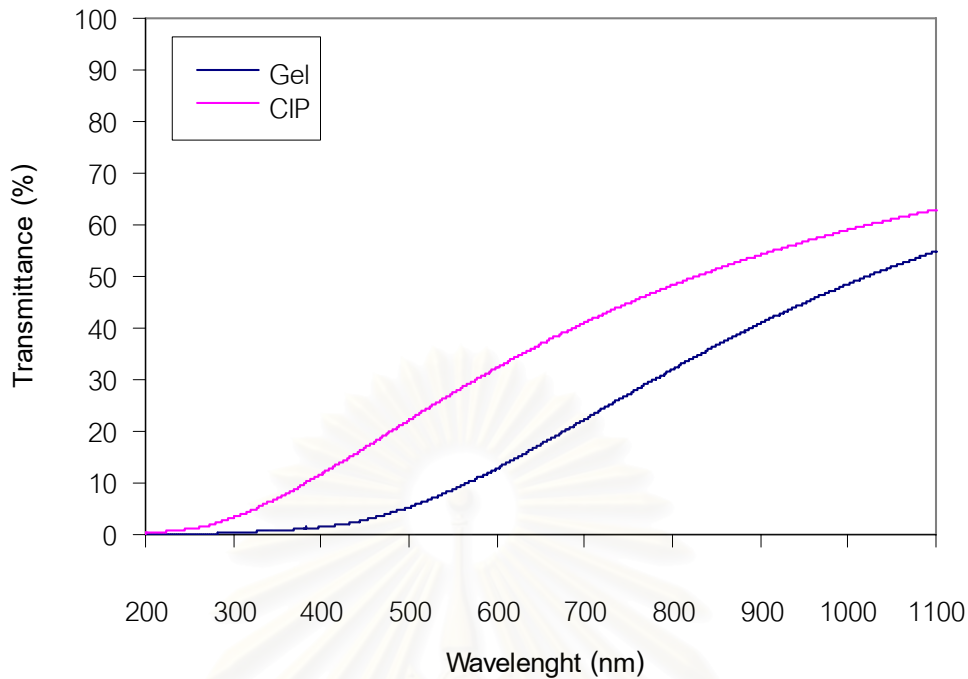


Fig.4.29 Relationship between wavelength and transmittance (%T) of HIPed specimens formed by gel-casting and CIP methods.

The transmittance value of Fig. 4.29 was lower than that of Fig. 4.16 even the thickness of specimen for Fig. 4.29 (0.8 mm) less than specimen for Fig. 4.16 (1.0 mm). The specimens for Fig. 4.16 were polished by a Japanese company. The surface roughness (Ra) of specimen for Fig. 4.16 is shown in appendix H. The specimens for Fig. 4.29 were polished in our department. The surface roughness of our specimens polished by us had not been measured. However, the appearance of the surfaces of specimens polished by the Japanese company were much smoother than ours. Consequently, we can conclude that one of the cause of the difference in transmittance was the difference of surface polishing.

## CHAPTER V

### CONCLUSIONS

The aim of this study was to develop a technology for synthesizing transparent polycrystalline alumina ceramics. The conclusions are as follows:

1. MgO contents did not affect the densities of sintered specimens, but affect the color of sintered specimens. When magnesia (MgO) was added to alumina and sintered in air, the color turned to yellow. But turned to gray, when sintered under vacuum. When MgO-free alumina was sintered in air and under vacuum, the color turned to white and pale-gray, respectively.
2. The sintering atmosphere played an important role in achieving a full density. When MgO-free and MgO doped alumina sintered in air atmosphere, full density was not obtained. While, sintered under vacuum, full density was obtained.
3. Grain size of specimens sintered in air atmosphere was smaller than that under vacuum at the same sintering temperature. Nanometer size grain was achieved at sintering temperature lower than 1350°C. However, full densities was not obtained, so hot isostatic pressing (HIPing) was essential to attain full density for the specimen sintered in air.
4. Specimen pre-sintered in air atmosphere followed by hot isostatic pressing became transparent. On the other hand, specimen pre-sintered under vacuum was translucent and it was still showed gray color after HIP. After heat treatment, the color of specimen pre-sintered under vacuum followed by HIPing changed from translucent gray to translucent and that of pre-sintered in air changed from transparent to transparent yellow.

5. The optimum amount of dispersant for 65, 70 and 75 wt.% of pure alumina slurries were 1.0, 1.3 and 1.6 wt.% based on dry solid, respectively. After adding  $Mg(NO_3)_2 \cdot 6H_2O_{(s)}$  to the slurries with minimum viscosity for each solid loading, the viscosity of slurries increased. Then, dispersant was added more. The optimum amount of dispersant for 65, 70 and 75 wt.% alumina slurries increased to 1.3, 1.7 and 1.9 wt.%, respectively.
6. A suitable condition for gel-casting using agar as gelling additive depended not only on the viscosity of slurry, but also on the dimension and shape of obtained bodies. Drying in closed chamber exhibited better dimension than drying in open air according to the uniformity of shrinkage direction.
7. Density of dried bodies increased with increasing alumina contents. On the other hand, in all cases the density tends to decrease when total concentration of agar increased. From these result, 75 wt% alumina powder and 0.1 wt% agar composition had highest green density due to highest solid content.
8. Sintered alumina formed by gel casting method showed transparency. However, specimens formed by CIP method showed better transparency than that formed by gel casting method.

## CHAPTER VI

### FUTURE WORKS

In this research, transparent alumina ceramics composed of nanometer size grain could be made. However, sintering conditions should be studied more to obtain a specimen with higher transmittance. The future works are recommended as follows:

1. To obtain better transparency, gel casting process should be researched in more detail. For example, (1) Nano-size MgO powder is substituted to  $Mg(NO_3)_2 \cdot 6H_2O_{(s)}$ , because adding  $Mg(NO_3)_2 \cdot 6H_2O_{(s)}$  the viscosity of slurry increased. (2) Best sintering time should be surveyed and (3) BN crucible should be used as the container in HIP.
2. To increase the densification rate, novel sintering technique such as vacuum sintering (without carbon heater and  $P_{O_2}$  controlled), hydrogen atmosphere sintering and microwave sintering should be studied.
3.  $Al_2O_3$  powders with color dopants should be synthesized and used to obtain colored transparent  $Al_2O_3$ .

สถาบันวิทยบริการ  
จุฬาลงกรณ์มหาวิทยาลัย

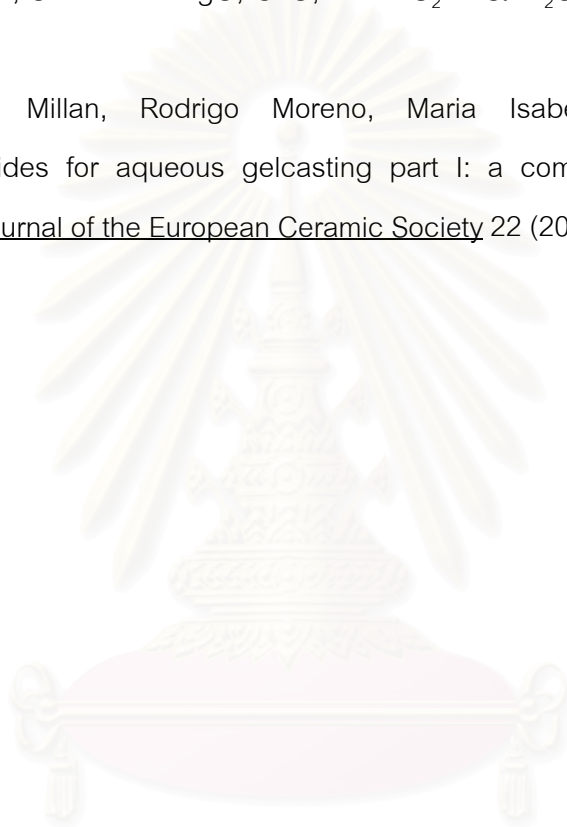
## REFERENCES

1. E. Ryshkewitch. Oxide Ceramics. New York : Academic Press, 1960.
2. W.H. Gitzen. Alumina as a Ceramic Material. The American Ceramic Society ISBN 0916094464.
3. E. Dörre, H.Hübner. Alumina, Processing, Properties, and Applications. Berlin, Heidelberg, New York, Tokyo : Springer-Verlag,1984.
4. C. A. Handwerker, R. M. Cannon and R. H. French, Robert L. Coble: A Retrospective, J. Am. Ceram. Soc. 77, 2 (1994): 293-298.
5. Jiping Cheng, Dinesh Agrawal, Yunjin Zhang, Rustum Roy. Microwave sintering of transparent alumina. Materials letters. 56 (2002): 587-592.
6. R. L. Coble. Transparent Alumina and Method of Preparation. U.S. Pat. No. 3 026 210 (1962).
7. K. Hayashi, O. Kobayashi, S. Toyoda, and K. Morinaga. Transmission Optical Properties of Polycrystalline Alumina with Submicron Grains. Mater. Trans. JIM, 32 (1991): 1024-1029.
8. R. Apetz and Van Broggen. Transparent Alumina: A Light-Scattering Model. J. Am. Ceram. Soc. 86, 3 (2003): 480-486.
9. Y.T. O and J.B. Koo. Effect of grain size on transmittance and mechanical strength of sintered alumina. Materials Science and Engineering A 374 (2004):191-195.
10. Krell, A. and Blank, P., Grain size dependence of hardness in dense submicrometer alumina. J. Am. Ceram. Soc. 78 (1995): 1118-1120.
11. Andreas Krell and Paul Blank. The Influence of Shaping Method on Grain Size Dependence of Strength in Dense Submicrometre. Journal of the European Ceramic Society 16 (1996):1189-1200.
12. Michel W. Barsoum. Fundamentals of Ceramics. New York : The McGraw-Hill, (1997).
13. N. Grimm, G E. Scott, and J. D. Sibold. Infrared Transmission Properties of High-Density Alumina. Am. Ceram. Soc. Bull. 50 (1971): 962-965.

14. K. Hayashi, O. Kabayashi, S. Toyoda, and K. Morinaga. Transmission Optical Properties of Polycrystalline Alumina with Submicron Grains. Mater. Trans. JIM, 32 (1991): 1024-1029.
15. M. E. Thomas, S. K. Andersson, R. M. Sova, and R. I. Joseph. Frequency and Temperature Dependence of the Refractive Index of Sapphire. Infrared Phys. Techno. 39, 4 (1998): 235-249.
16. M. Born and E. Wolf. Principle of Optics. Oxford, U.K : Pergamon Press, (1975).
17. Krell, A., Fracture origin and strength in advanced pressureless sintered alumina. J. Am. Ceram. Soc. 81 (1998): 1900-1906.
18. Li, J. G. and Sun, X. Synthesis and sintering behaviour of a nanocrystalline  $\alpha$ -alumina powder. Acta Mater. 48 (1998): 3103-3112.
19. Rao, P., Iwasa, M. and Kondoh, I., Properties of low-temperature sintered high purity  $\alpha$ -alumina ceramics. J. Mater. Sci. Lett. 19 (2000): 543-545.
20. Tari, G., Ferreira, J. M. F., Fonseca, A. T. and Lyckfeldt. O., Influence of particle size distribution on colloidal processing of alumina. J. Eur. Ceram. Soc. 18 (1998): 249-253.
21. E. W. Golibersuch. Method of Making Cemented Carbide Articles and Articles Produced Thereby. Can. Pat. No. 642 217 (1962).
22. O. Omatete, M. A. Janney, and R. A. Strehlow. Gelcasting – A New Ceramic Forming Process for Ceramic Powders. Am. Ceram. Soc. Bull. 70, 10 (1991): 1641-1649.
23. M. A. Janney, O.O. Omatete, C.A. Walls, S. D. Nunn, R. J. Ogle and G. Westmoreland. Development of Low-Toxicity Gelcasting Systems. J. Am. Ceram. Soc. 81, 3 (1998): 581-591.
24. P. R. Chu, and J. K. Cochran. UV Polymerization of Aqueous Slurries for Application in Ceramic Processing. Paper No. XVIIb-81-94, Presented at 96th Annual Meeting of Am. Ceram. Soc., Indianapolis, IN, 1994.
25. S. L. Morissette and J. A. Lewis. Chemorheology of Aqueous Alumina-Poly(Vinyl Alcohol) Gelcasting Suspension. J. Am. Ceram. Soc. 82, 3 (1999) 521-528.
26. N. McN. Alford, J. D. Brichall, and K. Kedall: Nature, (1987):330-51. F. F. Lange: J. Am. Ceram. Soc. (1989): 72-73.

27. Coble, R.L. Sintering Crystalline solid: I, Intermediate and final state diffusion models. J. Appl.Phys. 32 (1961): 787-792.
28. K. Morinaga, T. Torikai. K. Nakagawa, and S. Fujino. Fabrication of Fine  $\alpha$ -Alumina Powders by Thermal Decomposition of Ammonium Aluminium Carbonate Hydroxide (AACH). Acta Mater. 48,18/19 (2000): 4735-4741.
29. A.G. Evans and C.H. Hsueh, Behavior of large Pores during Sintering and Hot Isostatic Pressing. J. Am. Ceram. Soc. 69, 6 (1986): 444-448.
30. R. L. Coble. Sintering Polycrystalline Solid. J. Appl. Phys. 32 (1961): 787-99.
31. P. Hing. Vacuum Sintering of Aluminium Oxide to Translucency. Novel Synthesis and Processing of Ceramic, British Ceramic Processing. 53 (1994): 145-168.
32. G. C. Wei and W. H. Rhodes. Sintering of Translucent Alumina in a Nitrogen-Hydrogen Gas Atmosphere. J. Am. Ceram. Soc. 83, 7 (2000): 1641-1648.
33. J. G. J. Peelen and R. Metselaar. Light Scattering by Pores in Polycrystalline Materials: Transmission Properties of Alumina. J. Appl. Phys. 45, 1 (1974): 216-220.
34. J. G. J. Peelen. Transparent Hot-Pressed Alumina: II, Transparent versus Translucent Alumina. Ceramurgia Int. 5, 3 (1979): 115-119.
35. H. Mizuta, K. Oda, Y. Shibasaki, M. Maeda, M. Machida, and K. Ohshima. Preparation of High-Strength and Translucent Alumina by Hot Isostatic Pressing. J. Am. Ceram. Soc. 75, 2 (1992): 469-473.
36. Y. Hotta, T. Tsugoshi, and T. Nagao Effects of oligosaccharide alcohol addition to slurry an translucent alumina produced by slip casting. J. Am. Ceram. Soc. 86, 5 (2003) 755-760.
37. D. Godlinski, M. Kuntz, and G. Grathwohl, Transparent alumina with submicrometer grains by float packing and sintering. J. Am. Ceram. Soc. 85, 10 (2002): 2449-2456.
38. Andreas Kreel and Pual Blank. Transparent Sintered Corundum with High-Hardness and Strength. J. Am. Ceram. Soc. 86, 1 (2003): 12-18.
39. James S. Reed. Principles of ceramics processing. John wiley & Sons, Inc, 2<sup>nd</sup> edition, 1995.
40. Jim C. Thermal stability of the group 2 carbonates and nitrates [online] Available from: <http://www.chemguide.co.uk/inorganic/group2/thermstab.html> [10 june 2005]

41. A. L. Ivanovskii and G. P. Shveikin, Quantum Chemistry in Materials Science. Nonmetallic High-Melting Compounds and Nonmetallic Ceramics [in Russian]. Izd. 2-“Ekaterinburg,” Ekaterinburg (2000).
42. A. Stashans, E. A. Kotomin, and J. L. Calais, Calculation of the ground and excited states of F-type centers in corundum crystals. Phys. Rev. 49, 21 (1994): 14854 – 14858.
43. R. W. Grimes, Solution of MgO, CaO, and TiO<sub>2</sub> in  $\alpha$ -Al<sub>2</sub>O<sub>3</sub>, J. Am. Ceram. Soc. 77, (1994): 378.
44. Arnaldo J. Millan, Rodrigo Moreno, Maria Isabel Nieto, Thermogelling polysaccharides for aqueous gelcasting part I: a comparative study of gelling additives. Journal of the European Ceramic Society 22 (2002): 2209-2215



สถาบันวิทยบริการ  
จุฬาลงกรณ์มหาวิทยาลัย





APPENDICES

สถาบันวิทยบริการ  
จุฬาลงกรณ์มหาวิทยาลัย

## Appendix A. Density of green bodies formed by biaxial press method.

Sample	W	Ø	Thick	B.D.(g/cc)	RD (%)
TR1/1	2.7352	2.545	0.255	2.11	53.0
2	2.7534	2.545	0.25	2.17	54.4
3	2.7509	2.545	0.255	2.12	53.3
Avg.				2.13	53.6
S.D.				0.03	0.75

Sample	W	Ø	Thick	B.D.(g/cc)	RD (%)
TR2/1	2.7197	2.545	0.255	2.10	52.7
2	2.7415	2.545	0.25	2.16	54.2
3	2.7422	2.545	0.255	2.12	53.1
Avg.				2.12	53.3
S.D.				0.0	0.76

Sample	W	Ø	Thick	B.D.(g/cc)	RD (%)
TR3/1	2.7478	2.545	0.255	2.12	53.2
2	2.7243	2.545	0.255	2.10	52.8
3	2.7404	2.545	0.255	2.11	53.1
Avg.				2.11	53.1
S.D.				0.0	0.23

Sample	W	Ø	Thick	B.D.(g/cc)	RD (%)
TR4/1	2.7064	2.545	0.25	2.13	53.5
2	2.7409	2.545	0.255	2.11	53.1
3	2.7385	2.545	0.255	2.11	53.1
Avg.				2.12	53.2
S.D.				0.01	0.23

Sample	W	Ø	Thick	B.D.(g/cc)	RD (%)
TR5/1	2.6825	2.545	0.25	2.11	53.0
2	2.7739	2.545	0.255	2.14	53.8
3	2.7157	2.545	0.25	2.14	53.7
Avg.				2.13	53.5
S.D.				0.02	0.40

Appendix B. Density of green bodies formed by CIP method.

Sample	W	$\varnothing$	Thick	B.D.(g/cc)	RD (%)
TR1/1	3.3558	2.46	0.31	2.28	57.3
2	3.3757	2.465	0.315	2.25	56.5
3	3.3734	2.46	0.315	2.25	56.6
Avg.				2.26	56.8
S.D.				0.02	0.42

Sample	W	$\varnothing$	Thick	B.D.(g/cc)	RD (%)
TR2/1	2.7412	2.45	0.26	2.24	56.2
2	2.7185	2.43	0.26	2.26	56.7
3	3.1330	2.45	0.29	2.29	57.6
Avg.				2.26	56.8
S.D.				0.03	0.71

Sample	W	$\varnothing$	Thick	B.D.(g/cc)	RD (%)
TR3/1	2.7279	2.43	0.26	2.26	56.9
2	2.7216	2.44	0.26	2.24	56.3
3	2.7254	2.43	0.26	2.26	56.8
Avg.				2.25	56.7
S.D.				0.01	0.33

Sample	W	$\varnothing$	Thick	B.D.(g/cc)	RD (%)
TR4/1	2.7498	2.44	0.26	2.26	56.9
2	2.7196	2.45	0.26	2.22	55.8
3	2.7301	2.45	0.26	2.23	56.0
Avg.				2.24	56.2
S.D.				0.02	0.57

Sample	W	$\varnothing$	Thick	B.D.(g/cc)	RD (%)
TR5/1	2.7376	2.45	0.26	2.23	56.1
2	2.7368	2.45	0.26	2.23	56.1
3	2.7359	2.44	0.26	2.25	56.6
Avg.				2.24	56.3
S.D.				0.01	0.25

Appendix B (Cont.). Density of green bodies formed by CIP (Measurement by Archimedes' method)

Sample	D(g)	S(g)	W(g)	A.P.(%)	W.A.(%)	A.D.(g/cc)	B.D.(g/cc)	R.D.(%)
TR3/1	2.7224	2.0349	3.238	42.86	18.94	3.95	2.26	56.7
2	2.7165	2.0315	3.2306	42.87	18.93	3.95	2.26	56.8
3	2.7257	2.0375	3.2422	42.87	18.95	3.95	2.26	56.7
<b>Avg.</b>	<b>2.7215</b>	<b>2.0346</b>	<b>3.2369</b>	<b>42.87</b>	<b>18.94</b>	<b>3.95</b>	<b>2.26</b>	<b>56.7</b>
S.D.	0.005	0.003	0.006	0.0	0.01	0.003	0.002	0.04



สถาบันวิทยบริการ  
จุฬาลงกรณ์มหาวิทยาลัย

Appendix C. Bulk density, relative density, apparent porosity and water absorption of  
CIP specimens sintered under vacuum atmosphere

1250°C

Sample	D(g)	S(g)	W(g)	A.P.(%)	W.A.(%)	A.D.(g/cc)	B.D.(g/cc)	R.D.(%)
TR1-1	2.5944	1.9197	2.5963	0.28	0.07	3.84	3.83	96.0
TR1-2	2.5875	1.9139	2.5895	0.30	0.08	3.83	3.82	95.9
TR1-3	2.6304	1.9446	2.6312	0.12	0.03	3.83	3.82	95.9
Avg.				0.23	0.06	3.83	3.82	95.9
S.D.				0.10	0.03	0.00	0.00	0.06
TR2-1	2.7101	2.0069	2.7141	0.57	0.15	3.85	3.82	95.9
TR2-2	2.7045	2.0027	2.7089	0.62	0.16	3.85	3.82	95.8
TR2-3	2.7144	2.0105	2.7188	0.62	0.16	3.85	3.82	95.9
Avg.				0.60	0.16	3.85	3.82	95.9
S.D.				0.03	0.01	0.00	0.00	0.04
TR3-1	2.7128	2.0077	2.7143	0.21	0.06	3.84	3.83	96.1
TR3-2	2.7015	1.9994	2.7034	0.27	0.07	3.84	3.83	96.0
TR3-3	2.6935	1.9928	2.6953	0.26	0.07	3.84	3.82	96.0
Avg.				0.25	0.06	3.84	3.83	96.0
S.D.				0.03	0.01	0.00	0.00	0.06
TR4-1	2.7238	2.0181	2.7262	0.3	0.09	3.85	3.84	96.3
TR4-2	2.6695	1.9736	2.6721	0.4	0.10	3.83	3.81	95.6
TR4-3	2.7013	2.0003	2.7042	0.4	0.11	3.85	3.83	96.0
Avg.				0.4	0.10	3.84	3.83	96.0
S.D.				0.04	0.01	0.01	0.01	0.32
TR5-1	2.7038	1.982	2.7072	0.5	0.13	3.74	3.72	93.3
TR5-2	2.746	2.0125	2.7503	0.6	0.16	3.74	3.71	93.1
TR5-3	2.6998	1.9837	2.7021	0.3	0.09	3.76	3.75	94.0
Avg.				0.5	0.12	3.75	3.73	93.5
S.D.				0.13	0.04	0.01	0.02	0.48

สถาบันวิทยบริการ  
จุฬาลงกรณ์มหาวิทยาลัย

1300°C

Sample	D(g)	S(g)	W(g)	A.P.(%)	W.A.(%)	A.D.(g/cc)	B.D.(g/cc)	R.D.(%)
TR1-1	2.6129	1.9531	2.6137	0.12	0.03	3.95	3.95	99.0
TR1-2	2.6155	1.9549	2.6165	0.15	0.04	3.95	3.94	98.9
TR1-3	2.5116	1.8771	2.5119	0.05	0.01	3.95	3.95	99.0
Avg.				0.11	0.03	3.95	3.95	99.0
S.D.				0.05	0.01	0.001	0.002	0.04
TR2-1	3.1846	2.3808	3.1856	0.12	0.03	3.95	3.95	99.0
TR2-2	2.7037	2.0213	2.7049	0.18	0.04	3.95	3.95	99.0
TR2-3	2.7373	2.0465	2.738	0.10	0.03	3.95	3.95	99.1
Avg.				0.13	0.03	3.95	3.95	99.0
S.D.				0.04	0.01	0.000	0.002	0.04
TR3-1	2.6902	2.0146	2.6905	0.0	0.01	3.97	3.97	99.6
TR3-2	2.6997	2.0212	2.7000	0.0	0.01	3.97	3.97	99.5
TR3-3	2.7112	2.0304	2.7117	0.1	0.02	3.97	3.97	99.6
Avg.				0.05	0.01	3.97	3.97	99.6
S.D.				0.02	0.00	0.002	0.002	0.04
TR4-1	2.6864	2.0102	2.6869	0.07	0.02	3.96	3.96	99.3
TR4-2	2.7294	2.0428	2.7306	0.17	0.04	3.97	3.96	99.3
TR4-3	2.6851	2.0096	2.6855	0.06	0.01	3.97	3.96	99.4
Avg.				0.10	0.03	3.97	3.96	99.4
S.D.				0.06	0.02	0.001	0.002	0.055
TR5-1	2.6855	2.0091	2.6865	0.15	0.04	3.96	3.95	99.2
TR5-2	2.6988	2.0195	2.7009	0.31	0.08	3.96	3.95	99.1
TR5-3	2.7124	2.0301	2.7134	0.15	0.04	3.97	3.96	99.3
Avg.				0.20	0.05	3.96	3.96	99.2
S.D.				0.09	0.02	0.003	0.004	0.11

สถาบันวิทยบริการ  
จุฬาลงกรณ์มหาวิทยาลัย

1350°C

Sample	D(g)	S(g)	W(g)	A.P.(%)	W.A.(%)	A.D.(g/cc)	B.D.(g/cc)	R.D.(%)
TR1-1	2.5962	1.942	2.5968	0.09	0.02	3.96	3.96	99.3
TR1-2	2.6245	1.9647	2.6250	0.08	0.02	3.97	3.97	99.5
TR1-3	2.5372	1.8988	2.5374	0.03	0.01	3.97	3.97	99.5
Avg.				0.07	0.02	3.97	3.96	99.4
S.D.				0.03	0.01	0.00	0.01	0.13
TR2-1	2.6918	2.0169	2.6923	0.07	0.02	3.98	3.98	99.8
TR2-2	2.7072	2.0268	2.7075	0.04	0.01	3.97	3.97	99.6
TR2-3	2.7249	2.041	2.7258	0.13	0.03	3.98	3.97	99.6
Avg.				0.08	0.02	3.98	3.97	99.7
S.D.				0.04	0.01	0.00	0.00	0.11
TR3-1	2.7095	2.03	2.7099	0.06	0.01	3.98	3.98	99.8
TR3-2	2.7024	2.0249	2.7033	0.13	0.03	3.98	3.98	99.7
TR3-3	2.7059	2.0276	2.7068	0.13	0.03	3.98	3.98	99.7
Avg.				0.11	0.03	3.98	3.98	99.8
S.D.				0.04	0.01	0.00	0.00	0.02
TR4-1	2.7309	2.046	2.7311	0.03	0.01	3.98	3.98	99.8
TR4-2	2.7006	2.023	2.7007	0.01	0.00	3.98	3.98	99.8
TR4-3	2.7105	2.0307	2.7115	0.15	0.04	3.98	3.97	99.7
Avg.				0.06	0.02	3.98	3.98	99.8
S.D.				0.07	0.02	0.00	0.00	0.06
TR5-1	2.7169	2.0338	2.7173	0.06	0.01	3.97	3.97	99.5
TR5-2	2.7167	2.0346	2.7171	0.06	0.01	3.97	3.97	99.7
TR5-3	2.7153	2.0352	2.7156	0.04	0.01	3.98	3.98	99.9
Avg.				0.05	0.01	3.98	3.97	99.7
S.D.				0.01	0.00	0.01	0.01	0.20

สถาบันวิทยบริการ  
จุฬาลงกรณ์มหาวิทยาลัย

1450°C

Sample	D(g)	S(g)	W(g)	A.P.(%)	W.A.(%)	A.D.(g/cc)	B.D.(g/cc)	R.D.(%)
TR1-1	2.5663	1.9224	2.5672	0.14	0.04	3.98	3.97	99.6
TR1-2	2.6032	1.9419	2.6033	0.02	0.00	3.93	3.93	98.5
TR1-3	2.6467	1.9813	2.6475	0.12	0.03	3.97	3.96	99.4
Avg.				0.09	0.02	3.96	3.95	99.2
S.D.				0.07	0.02	0.03	0.02	0.59
TR2-1	2.7242	2.0414	2.7244	0.03	0.01	3.98	3.98	99.8
TR2-2	2.7015	2.0254	2.7019	0.06	0.01	3.99	3.98	99.9
TR2-3	3.1142	2.3342	3.1146	0.05	0.01	3.98	3.98	99.9
Avg.				0.05	0.01	3.98	3.98	99.9
S.D.				0.02	0.00	0.00	0.00	0.06
TR3-1	2.7087	2.0309	2.7086	-0.01	0.00	3.99	3.99	100
TR3-2	2.7101	2.0318	2.7102	0.01	0.00	3.99	3.99	100
TR3-3	2.7048	2.0278	2.7054	0.09	0.02	3.99	3.98	99.9
Avg.				0.03	0.01	3.99	3.98	100
S.D.				0.05	0.01	0.00	0.00	0.07
TR4-1	2.6976	2.0221	2.6977	0.01	0.00	3.98	3.98	99.9
TR4-2	2.7040	2.029	2.7047	0.10	0.03	4.00	3.99	100
TR4-3	2.7197	2.0386	2.7207	0.15	0.04	3.98	3.98	99.8
Avg.				0.09	0.02	3.99	3.98	100
S.D.				0.07	0.02	0.01	0.01	0.18
TR5-1	2.7074	2.0294	2.7075	0.01	0.00	3.98	3.98	99.9
TR5-2	2.704	2.0287	2.7047	0.10	0.03	3.99	3.99	100
TR5-3	2.73	2.0458	2.7308	0.12	0.03	3.98	3.98	99.7
Avg.				0.08	0.02	3.99	3.98	99.9
S.D.				0.06	0.01	0.01	0.01	0.18

สถาบันวิทยบริการ  
จุฬาลงกรณ์มหาวิทยาลัย



1550°C

Sample	D(g)	S(g)	W(g)	A.P.(%)	W.A.(%)	A.D.(g/cc)	B.D.(g/cc)	R.D.(%)
TR1-1	2.5877	1.9389	2.5887	0.15	0.04	3.98	3.97	99.6
TR1-2	2.6211	1.9646	2.6225	0.21	0.05	3.98	3.97	99.7
TR1-3	2.6235	1.9652	2.624	0.08	0.02	3.97	3.97	99.6
Avg.				0.15	0.04	3.98	3.97	99.7
S.D.				0.07	0.02	0.00	0.00	0.03
TR2-1	2.7021	2.0258	2.7025	0.06	0.01	3.99	3.98	99.9
TR2-2	2.6854	2.0129	2.6860	0.09	0.02	3.98	3.98	99.8
TR2-3	2.7137	2.034	2.7143	0.09	0.02	3.98	3.98	99.8
Avg.				0.08	0.02	3.98	3.98	99.9
S.D.				0.02	0.00	0.00	0.00	0.05
TR3-1	2.7272	2.045	2.7274	0.03	0.01	3.99	3.99	100
TR3-2	2.6887	2.0157	2.6892	0.07	0.02	3.99	3.98	100
TR3-3	2.7012	2.0249	2.7014	0.03	0.01	3.98	3.98	99.9
Avg.				0.04	0.01	3.99	3.98	100
S.D.				0.03	0.01	0.00	0.00	0.06
TR4-1	2.7231	2.0402	2.7237	0.09	0.02	3.98	3.97	99.7
TR4-2	2.6987	2.024	2.6987	0.00	0.00	3.99	3.99	100
TR4-3	3.0278	2.27	3.0283	0.07	0.02	3.99	3.98	99.9
Avg.				0.05	0.01	3.98	3.98	100
S.D.				0.05	0.01	0.01	0.01	0.20
TR5-1	2.6984	2.0202	2.699	0.09	0.02	3.97	3.97	99.5
TR5-2	2.6678	1.9997	2.6679	0.01	0.00	3.98	3.98	100
TR5-3	2.7006	2.0242	2.7009	0.04	0.01	3.98	3.98	99.9
Avg.				0.05	0.01	3.98	3.98	99.8
S.D.				0.04	0.01	0.01	0.01	0.24

สถาบันวิทยบริการ  
จุฬาลงกรณ์มหาวิทยาลัย

Appendix D. Bulk density, relative density, apparent porosity and water absorption of CIP specimens sintered in air atmosphere for 2 h.

1250°C

Sample	D(g)	S(g)	W(g)	A.P.(%)	W.A.(%)	A.D.(g/cc)	B.D.(g/cc)	R.D.(%)
TR1-1	2.5684	1.9043	2.602	4.82	1.31	3.86	3.67	92.3
TR1-2	2.5659	1.9029	2.6054	5.62	1.54	3.86	3.64	91.5
TR1-3	2.5602	1.8955	2.5923	4.61	1.25	3.84	3.67	92.1
Avg.				5.02	1.37	3.86	3.66	92.0
S.D.				0.54	0.15	0.01	0.01	0.38
TR2-1	2.5911	1.9245	2.627	5.11	1.39	3.88	3.68	92.3
TR2-2	2.5888	1.9226	2.6262	5.32	1.44	3.88	3.67	92.1
TR2-3	2.5718	1.9092	2.6088	5.29	1.44	3.87	3.67	92.0
Avg.				5.24	1.42	3.88	3.67	92.1
S.D.				0.11	0.03	0.003	0.006	0.16
TR3-1	2.5911	1.9245	2.627	5.11	1.39	3.88	3.68	92.3
TR3-2	2.5888	1.9226	2.6262	5.32	1.44	3.88	3.67	92.1
TR3-3	2.5718	1.9092	2.6088	5.29	1.44	3.87	3.67	92.0
Avg.				5.24	1.42	3.88	3.67	92.1
S.D.				0.11	0.03	0.00	0.01	0.16
TR4-1	2.544	1.8901	2.5828	5.6	1.53	3.88	3.66	91.9
TR4-2	2.6099	1.941	2.6522	5.9	1.62	3.89	3.66	91.8
TR4-3	2.6242	1.9405	2.6632	5.4	1.49	3.83	3.62	90.9
Avg.				5.6	1.54	3.87	3.65	91.5
S.D.				0.28	0.07	0.03	0.02	0.58
TR5-1	2.6199	1.9398	2.6636	6.0	1.67	3.84	3.61	90.6
TR5-2	2.6	1.9245	2.6438	6.1	1.68	3.84	3.61	90.5
TR5-3	2.5719	1.9203	2.6166	6.4	1.74	3.94	3.68	92.4
Avg.				6.2	1.70	3.87	3.63	91.2
S.D.				0.21	0.04	0.06	0.04	1.11

จุฬาลงกรณ์มหาวิทยาลัย

1300°C

Sample	D(g)	S(g)	W(g)	A.P.(%)	W.A.(%)	A.D.(g/cc)	B.D.(g/cc)	R.D.(%)
TR1-1	2.5722	1.9133	2.573	0.12	0.03	3.90	3.89	97.6
TR1-2	2.5506	1.8999	2.5516	0.15	0.04	3.91	3.90	97.9
TR1-3	2.6065	1.9387	2.6077	0.18	0.05	3.90	3.89	97.5
Avg.				0.15	0.04	3.90	3.89	97.7
S.D.				0.03	0.01	0.01	0.01	0.24
TR2-1	2.5063	1.8667	2.5076	0.20	0.05	3.91	3.90	97.9
TR2-2	2.5770	1.9168	2.5787	0.26	0.07	3.90	3.88	97.4
TR2-3	2.5621	1.9055	2.5629	0.12	0.03	3.89	3.89	97.5
Avg.				0.19	0.05	3.90	3.89	97.6
S.D.				0.07	0.02	0.01	0.01	0.23
TR3-1	2.7179	2.0264	2.7214	0.5	0.13	3.92	3.90	97.9
TR3-2	2.7018	2.0107	2.7020	0.0	0.01	3.90	3.90	97.8
TR3-3	2.3207	1.725	2.3218	0.2	0.05	3.89	3.88	97.3
Avg.				0.24	0.06	3.90	3.89	97.8
S.D.				0.24	0.06	0.02	0.01	0.30
TR4-1	2.5783	1.9153	2.5791	0.12	0.03	3.88	3.87	97.2
TR4-2	2.6054	1.9406	2.6071	0.26	0.07	3.91	3.90	97.8
TR4-3	2.5886	1.9247	2.5894	0.12	0.03	3.89	3.88	97.5
Avg.				0.17	0.04	3.89	3.89	97.5
S.D.				0.08	0.02	0.02	0.01	0.31
TR5-1	2.6082	1.9385	2.6089	0.10	0.03	3.89	3.88	97.4
TR5-2	2.6443	1.9632	2.6447	0.06	0.02	3.87	3.87	97.1
TR5-3	2.5854	1.9193	2.5865	0.16	0.04	3.87	3.87	97.0
Avg.				0.11	0.03	3.88	3.87	97.1
S.D.				0.05	0.01	0.007	0.008	0.20

สถาบันวิทยบริการ  
จุฬาลงกรณ์มหาวิทยาลัย

1350°C

Sample	D(g)	S(g)	W(g)	A.P.(%)	W.A.(%)	A.D.(g/cc)	B.D.(g/cc)	R.D.(%)
TR1-1	2.7053	2.0231	2.7059	0.09	0.02	3.95	3.95	99.3
TR1-2	2.7172	2.0318	2.7180	0.12	0.03	3.95	3.95	99.2
TR1-3	2.7284	2.0401	2.7291	0.10	0.03	3.95	3.95	99.2
Avg.				0.10	0.03	3.95	3.95	99.2
S.D.				0.01	0.00	0.00	0.00	0.03
TR2-1	2.7119	2.0287	2.7125	0.09	0.02	3.96	3.96	99.4
TR2-2	2.7444	2.0512	2.745	0.09	0.02	3.95	3.94	99.1
TR2-3	2.7156	2.03	2.7162	0.09	0.02	3.95	3.95	99.2
Avg.				0.09	0.02	3.95	3.95	99.2
S.D.				0.00	0.00	0.01	0.01	0.14
TR3-1	2.6973	2.0189	2.698	0.10	0.03	3.96	3.96	99.5
TR3-2	2.7076	2.0265	2.7085	0.13	0.03	3.96	3.96	99.5
TR3-3	2.693	2.0151	2.6938	0.12	0.03	3.96	3.96	99.4
Avg.				0.12	0.03	3.96	3.96	99.5
S.D.				0.01	0.00	0.00	0.00	0.05
TR4-1	2.7095	2.0276	2.7102	0.10	0.03	3.96	3.96	99.5
TR4-2	2.7192	2.0334	2.7199	0.10	0.03	3.95	3.95	99.3
TR4-3	2.7508	2.0589	2.7511	0.04	0.01	3.97	3.96	99.6
Avg.				0.08	0.02	3.96	3.95	99.4
S.D.				0.03	0.01	0.01	0.01	0.17
TR5-1	2.6838	2.0073	2.6845	0.1	0.03	3.95	3.95	99.3
TR5-2	2.7656	2.0673	2.7664	0.1	0.03	3.95	3.95	99.1
TR5-3	2.6983	2.0175	2.6992	0.1	0.03	3.95	3.95	99.2
Avg.				0.12	0.03	3.95	3.95	99.2
S.D.				0.01	0.00	0.00	0.00	0.09

สถาบันวิทยบริการ  
จุฬาลงกรณ์มหาวิทยาลัย

1450°C

Sample	D(g)	S(g)	W(g)	A.P.(%)	W.A.(%)	A.D.(g/cc)	B.D.(g/cc)	R.D.(%)
TR1-1	2.7053	2.0231	2.7059	0.09	0.02	3.95	3.95	99.3
TR1-2	2.7172	2.0318	2.7180	0.12	0.03	3.95	3.95	99.2
TR1-3	2.7284	2.0401	2.7291	0.10	0.03	3.95	3.95	99.2
Avg.				0.10	0.03	3.95	3.95	99.2
S.D.				0.01	0.00	0.00	0.00	0.03
TR2-1	2.7119	2.0287	2.7125	0.09	0.02	3.96	3.96	99.4
TR2-2	2.7444	2.0512	2.745	0.09	0.02	3.95	3.94	99.1
TR2-3	2.7156	2.03	2.7162	0.09	0.02	3.95	3.95	99.2
Avg.				0.09	0.02	3.95	3.95	99.2
S.D.				0.00	0.00	0.006	0.005	0.14
TR3-1	2.6973	2.0189	2.698	0.10	0.03	3.96	3.96	99.5
TR3-2	2.7076	2.0265	2.7085	0.13	0.03	3.96	3.96	99.5
TR3-3	2.693	2.0151	2.6938	0.12	0.03	3.96	3.96	99.4
Avg.				0.12	0.03	3.96	3.96	99.5
S.D.				0.01	0.00	0.00	0.00	0.05
TR4-1	2.7095	2.0276	2.7102	0.10	0.03	3.96	3.96	99.5
TR4-2	2.7192	2.0334	2.7199	0.10	0.03	3.95	3.95	99.3
TR4-3	2.7508	2.0589	2.7511	0.04	0.01	3.97	3.96	99.6
Avg.				0.08	0.02	3.96	3.96	99.4
S.D.				0.03	0.01	0.008	0.007	0.17
TR5-1	2.6838	2.0073	2.6845	0.1	0.03	3.95	3.95	99.3
TR5-2	2.7656	2.0673	2.7664	0.1	0.03	3.95	3.95	99.1
TR5-3	2.6983	2.0175	2.6992	0.1	0.03	3.95	3.95	99.2
Avg.				0.12	0.03	3.95	3.95	99.2
S.D.				0.01	0.00	0.00	0.00	0.09

สถาบันวิทยบริการ  
จุฬาลงกรณ์มหาวิทยาลัย

1550°C

Sample	D(g)	S(g)	W(g)	A.P.(%)	W.A.(%)	A.D.(g/cc)	B.D.(g/cc)	R.D.(%)
TR1-1	2.6310	1.9695	2.6317	0.11	0.03	3.97	3.96	99.4
TR1-2	2.6134	1.9573	2.6145	0.17	0.04	3.97	3.97	99.5
TR1-3	2.6053	1.9487	2.6061	0.12	0.03	3.96	3.95	99.2
Avg.				0.13	0.03	3.97	3.96	99.4
S.D.				0.03	0.01	0.01	0.01	0.18
TR2-1	2.6077	1.9503	2.6085	0.12	0.03	3.96	3.95	99.1
TR2-2	2.6225	1.9621	2.6232	0.11	0.03	3.96	3.96	99.3
TR2-3	2.578	1.9292	2.5785	0.08	0.02	3.96	3.96	99.4
Avg.				0.10	0.03	3.96	3.96	99.3
S.D.				0.02	0.01	0.00	0.00	0.11
TR3-1	2.7885	2.0871	2.7892	0.10	0.03	3.97	3.96	99.4
TR3-2	2.8306	2.1172	2.8314	0.11	0.03	3.96	3.95	99.2
TR3-3	2.8928	2.1643	2.8937	0.12	0.03	3.96	3.96	99.3
Avg.				0.11	0.03	3.96	3.96	99.3
S.D.				0.01	0.00	0.00	0.00	0.11
TR4-1	2.5855	1.9345	2.5862	0.11	0.03	3.96	3.96	99.3
TR4-2	2.5720	1.9232	2.5729	0.14	0.03	3.95	3.95	99.1
TR4-3	2.5652	1.9204	2.5661	0.14	0.04	3.97	3.96	99.4
Avg.				0.13	0.03	3.96	3.96	99.3
S.D.				0.02	0.00	0.01	0.01	0.18
TR5-1	2.5777	1.9287	2.5786	0.14	0.03	3.96	3.96	99.3
TR5-2	2.6090	1.9511	2.6101	0.17	0.04	3.96	3.95	99.1
TR5-3	2.5839	1.9323	2.5846	0.11	0.03	3.96	3.95	99.1
Avg.				0.14	0.03	3.96	3.95	99.2
S.D.				0.03	0.01	0.00	0.00	0.09

สถาบันวิทยบริการ  
จุฬาลงกรณ์มหาวิทยาลัย

Appendix E. Average grain size of sintered specimens.

Sintering temperature	Average grain size (um)									
	TR1A	TR2A	TR3A	TR4A	TR5A	TR1V	TR2V	TR3V	TR4V	TR5V
1250°C								0.31		
1300°C										
1350°C	0.45	0.27	0.45	0.30	0.32	0.77		0.95	0.77	0.88
1450°C	2.18		0.94			2.3	1.33	1.04	1.25	1.17
1550°C							3.4	3.05	3.43	3.51



สถาบันวิทยบริการ  
จุฬาลงกรณ์มหาวิทยาลัย

Appendix F. Density of green bodies form by gel casting using agar as gelling additive.

Sample	D(g)	S(g)	W(g)	A.P.(%)	W.A.(%)	A.D.(g/cc)	B.D.(g/cc)	R.D.(%)
G2/1	4.534	3.3719	5.5601	46.9	22.6	3.89	2.07	51.9
2	3.715	2.7632	4.553	46.8	22.6	3.89	2.07	52.0
3	3.6882	2.7444	4.5178	46.8	22.5	3.90	2.07	52.1
Avg.	3.9791	2.9598	4.877	46.8	22.6	3.89	2.07	52.0
S.D.	0.48	0.36	0.59	0.10	0.07	0.01	0.00	0.10

Sample	D(g)	S(g)	W(g)	A.P.(%)	W.A.(%)	A.D.(g/cc)	B.D.(g/cc)	R.D.(%)
G3/1	3.7245	2.7729	4.595	47.8	23.4	3.90	2.04	51.2
2	3.8767	2.8854	4.7841	47.8	23.4	3.90	2.04	51.2
3	4.5069	3.356	5.5603	47.8	23.4	3.91	2.04	51.2
Avg.	4.036	3.0048	4.9798	47.8	23.4	3.90	2.04	51.2
S.D.	0.42	0.31	0.51	0.00	0.02	0.01	0.00	0.04

Sample	D(g)	S(g)	W(g)	A.P.(%)	W.A.(%)	A.D.(g/cc)	B.D.(g/cc)	R.D.(%)
G5C/1	4.8549	3.5991	5.8198	43.45	19.87	3.85	2.18	54.8
2	5.0328	3.7281	6.0308	43.34	19.83	3.85	2.18	54.8
3	4.5756	3.3971	5.4874	43.62	19.93	3.87	2.18	54.9
Avg.	4.8211	3.5748	5.7793	43.47	19.88	3.86	2.18	54.8
S.D.	0.23	0.17	0.27	0.10	0.05	0.02	0.00	0.04

Sample	D(g)	S(g)	W(g)	A.P.(%)	W.A.(%)	A.D.(g/cc)	B.D.(g/cc)	R.D.(%)
G5OP/1	4.5071	3.3384	5.3996	43.3	19.8	3.84	2.18	54.8
2	4.9568	3.6723	5.9353	43.24	19.74	3.85	2.18	54.9
3	4.79	3.54	5.73	43.18	19.73	3.84	2.18	54.8
Avg.	4.7503	3.5183	5.6887	43.24	19.76	3.84	2.18	54.8
S.D.	0.227	0.168	0.27	0.1	0.04	0.001	0.002	0.05

Sample	D(g)	S(g)	W(g)	A.P.(%)	W.A.(%)	A.D.(g/cc)	B.D.(g/cc)	R.D.(%)
G6C	3.7751	2.7954	4.5352	43.69	20.13	3.84	2.16	54.4
	3.9842	2.9477	4.7835	43.54	20.06	3.83	2.16	54.4
	3.9697	2.9432	4.7518	43.24	19.7	3.86	2.19	55.0
Avg.	3.91	2.90	4.69	43.49	19.97	3.84	2.17	54.6
S.D.	0.1170	0.087	0.135	0.2	0.23	0.014	0.01	0.36

Sample	D(g)	S(g)	W(g)	A.P.(%)	W.A.(%)	A.D.(g/cc)	B.D.(g/cc)	R.D.(%)
G6OP/1	4.0619	3.0037	4.8722	43.37	19.95	3.83	2.17	54.5
2	3.67	2.71	4.41	43.25	19.95	3.81	2.16	54.3
3	4.6038	3.4109	5.5239	43.54	19.99	3.85	2.17	54.6
Avg.	4.1134	3.0424	4.9346	43.39	19.96	3.83	2.17	54.5
S.D.	0.467	0.351	0.561	0.1	0.02	0.022	0.005	0.10



Appendix F. (Cont.) Density of green bodies form by gel casting using agar as gelling additive.

Sample	D(g)	S(g)	W(g)	A.P.(%)	W.A.(%)	A.D.(g/cc)	B.D.(g/cc)	R.D.(%)
G7/1	5.3770	3.9993	6.328	40.84	17.69	3.89	2.30	57.9
G7/2	5.4444	4.0296	6.4284	41.02	18.07	3.84	2.26	56.9
G7/3	6.5922	4.8922	7.7921	41.38	18.2	3.87	2.27	57.0
Avg.	5.8045	4.307	6.8495	41.08	17.99	3.87	2.28	57.2
S.D.	0.68	0.51	0.82	0.30	0.27	0.03	0.02	0.55

Sample	D(g)	S(g)	W(g)	A.P.(%)	W.A.(%)	A.D.(g/cc)	B.D.(g/cc)	R.D.(%)
G8/1	4.9241	3.6113	5.8435	41.19	18.67	3.74	2.2	55.3
G8/2	4.4313	3.2826	5.2654	42.07	18.82	3.85	2.23	56.0
G8/3	4.8147	3.5671	5.7131	41.86	18.66	3.85	2.24	56.2
Avg.	4.72	3.49	5.61	41.71	18.72	3.81	2.22	55.8
S.D.	0.2590	0.178	0.303	0.5	0.09	0.063	0.02	0.49

Sample	D(g)	S(g)	W(g)	A.P.(%)	W.A.(%)	A.D.(g/cc)	B.D.(g/cc)	R.D.(%)
G9/1	4.4859	3.324	5.34	42.37	19.04	3.85	2.22	55.8
G9/2	4.7054	3.483	5.5786	41.67	18.56	3.84	2.24	56.3
G9/3	4.6658	3.4586	5.5563	42.45	19.09	3.86	2.22	55.7
Avg.	4.62	3.42	5.49	42.16	18.89	3.85	2.22	55.9
S.D.	0.1170	0.086	0.132	0.4	0.29	0.01	0.01	0.3

Note: C = Drying in closed chamber and OP = Drying in an open air

สถาบันวิทยบริการ  
จุฬาลงกรณ์มหาวิทยาลัย

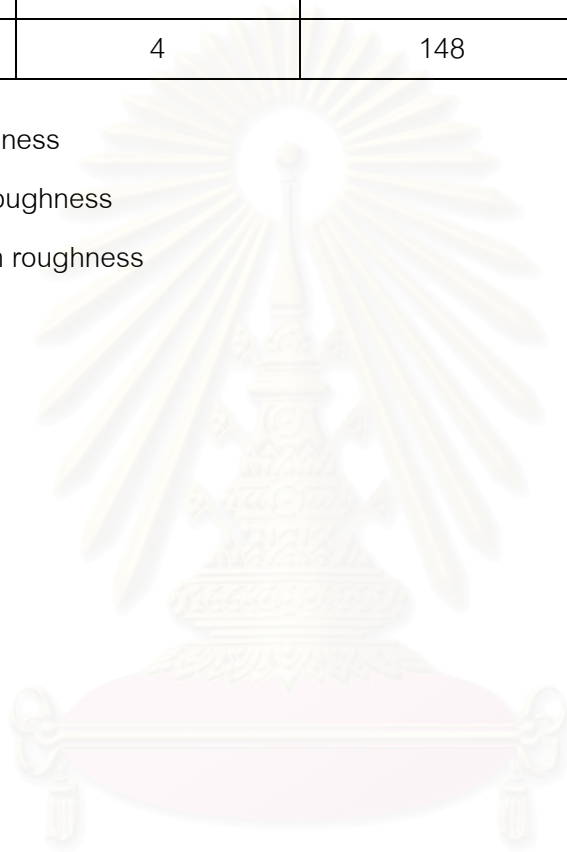
Appendix H. Surface roughness of specimens polished by a Japanese company.

Specimen	Ra (nm)	Rmax (nm)	Rz (nm)
TR2A	5	80	63
TR3A	7	170	92
TR4A	6	276	xxx
TR5A	4	148	xxx

Ra = Average roughness

Rmax = Maximum roughness

Rz= Mean maximum roughness



สถาบันวิทยบริการ  
จุฬาลงกรณ์มหาวิทยาลัย

## BIOGRAPHY

Mr. Soontorn Tansungnoen was born in Nakornratchasima on 2<sup>nd</sup> of June 1976. He received a Bachelor's Degree in Chemistry from Faculty of Science and Technology, Rajabhat Institute Nakornratchasima in 2000. During his Bachelor study, he was also working at Siam Research and Development Co., Ltd. (Siam Cement Group). After working for 6 years, he continued a further study in Master's degree in the field of Ceramic Technology at Chulalongkorn University from June 2003 and graduated at the end of September 2005.



สถาบันวิทยบริการ  
จุฬาลงกรณ์มหาวิทยาลัย